NASA TECHNICAL NOTE

NASA TN D-3385

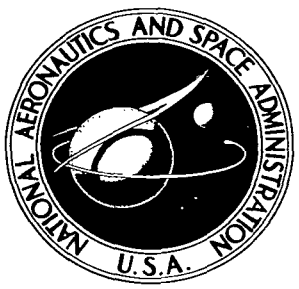

NASA TN D-3385

AN INVESTIGATION OF SPLITTER PLATES FOR THE AERODYNAMIC SEPARATION OF TWIN INLETS AT MACH 2.5

by George W. Moseley, John B. Peterson, Jr., and Albert L. Braslow

Langley Research Center
Langley Station, Hampton, Va.

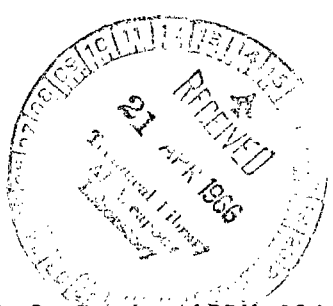

NATIONAL AERONAUTICS AND SPACE ADMINISTRATION • WASHINGTON, D. C. • APRIL 1966

NASA TN D-3385

AN INVESTIGATION OF SPLITTER PLATES FOR THE AERODYNAMIC SEPARATION OF TWIN INLETS AT MACH 2.5

By George W. Moseley, John B. Peterson, Jr.,
and Albert L. Braslow

Langley Research Center
Langley Station, Hampton, Va.

NATIONAL AERONAUTICS AND SPACE ADMINISTRATION

For sale by the Clearinghouse for Federal Scientific and Technical Information
Springfield, Virginia 22151 – Price $0.75

AN INVESTIGATION OF SPLITTER PLATES FOR THE AERODYNAMIC SEPARATION OF TWIN INLETS AT MACH 2.5

By George W. Moseley, John B. Peterson, Jr.,
and Albert L. Braslow
Langley Research Center

SUMMARY

An experimental investigation was conducted to determine the ability of various splitter plates to isolate twin inlets aerodynamically, so that, in the event one inlet is unstarted, the operation of the other inlet will not be affected. The effects of pylon height, inlet mass flow, and inlet yaw on the performance of the splitter plates were investigated. A pylon-mounted external-internal compression inlet model was used. The tests were made at a Mach number of 2.5 and a Reynolds number based on cowl diameter of 10.8×10^6, which are approximately full-scale flight conditions for an aircraft such as a supersonic transport.

It was determined that splitter plates of a practical size will isolate an unstarted inlet, at least as long as the mass-flow ratio is maintained above approximately 0.65. The effective splitter plates extended forward to the tip of the inlet centerbody, and the upper and lower edges of the plates extended above and below the cowl lip. An extension of 7.5 percent of the cowl diameter on the upper and lower edges was successful in preventing the unstarted flow field from spilling around the upper and lower edges. It was also found that splitter plates of practical size remained effective for yaw of the unstarted inlet to at least 6° windward and that pylon height had little effect on splitter-plate effectiveness except that at low heights where it was necessary that there be no gap between the splitter plate and the wing.

INTRODUCTION

The propulsion system of an aircraft such as a supersonic transport will be comprised of a number of propulsion packages, each consisting of an inlet, engine, and exhaust nozzle, and the optimum location of these propulsion packages relative to the wing and to one another is a consideration of extreme importance to aircraft performance and safety. This propulsion system is usually positioned underneath the wing in order to take advantage of the lower Mach number and of favorable interference effects which result when the shocks off the inlet cowl impinge on the lower surface of the wing and

create high-pressure regions. A number of investigations (ref. 1 and other proprietary investigations) have been conducted to determine the effects of various arrangements of the propulsion packages relative to one another.

Problems arise from the fact that inlet unstarts cannot presently be completely eliminated and that the unstart of one inlet must not initiate the unstart of an adjacent one, since two unstarted adjacent inlets would precipitate extreme rolling and yawing moments. An unstarted inlet will cause an unstart in an adjacent inlet when a sufficient amount of the flow spilling around the unstarted inlet enters the adjacent inlet. Also, the second inlet will suffer performance penalties if it continues to operate in the region of an unstarted inlet. Thus, it is desirable to locate the propulsion packages so that there is no interference between the inlets in the event of an unstart. This result may be accomplished by sufficient spanwise separation of the propulsion packages or by placing splitter plates or interference shields between the propulsion packages to block off any unstart and isolate the inlets (ref. 1).

Another proposed arrangement of the propulsion system which appears very promising is shown in figure 1 (taken from ref. 2). This arrangement places two propulsion packages in a single nacelle, and attempts to insure independent operation by employing a splitter plate which divides the nacelle, extends forward, and isolates the two inlets. There are a number of advantages to this configuration. First, the total wetted area of all the nacelles is reduced, and there are corresponding reductions in drag. Secondly, important benefits are obtained from the splitter plate which is used as a compression surface to decrease inlet size, increase inlet pressure recovery, and reduce flow distortions caused by yaw. In addition, the arrangement requires less space along the span of the wing than do arrangements with one engine per nacelle. This more compact arrangement is particularly desirable for variable-wing-sweep aircraft since it facilitates placement of the propulsion packages on the small fixed portion of the wing; in any case, placing the engines more nearly along the center line of an aircraft may be desirable simply for structural and aerodynamic reasons (for example, reduction in asymmetric thrust moment and reduction in roll moment of inertia).

These considerations make the twin-inlet arrangement a highly favorable design; however, the feasibility of the design hinges upon the ability of the splitter plate to isolate aerodynamically the two inlets so that in the event one inlet is unstarted, the operation of the other inlet will not be affected. This splitter plate must be of a practical size in order that the drag and weight of the plate will not override the advantages of the arrangement.

An investigation was conducted in the Langley 20-inch variable supersonic tunnel to determine the ability of splitter plates of practical size to isolate aerodynamically an unstarted twin-inlet model. The investigation was carried out at a Mach number of 2.5

and a Reynolds number based on cowl diameter of 10.8×10^6; these conditions are very near full-scale flight conditions for proposed supersonic transports. The effects of pylon height, yaw, and inlet mass flow on splitter-plate performance were also investigated.

SYMBOLS

Measurements for this investigation were taken in the U.S. Customary System of Units. Equivalent values in the International System (SI) are indicated herein in the interest of promoting use of this system in future NASA reports.

A_i inlet capture area, $\frac{1}{2}\frac{\pi D^2}{4}$, 9.82 in^2 (63.35 cm^2)

A_t inlet throat area, 5.10 in^2 (32.9 cm^2)

D cowl diameter, 5 in. (12.7 cm)

$\dot{m}_1$ mass-flow rate through stream tube of area A_i at conditions behind splitter plate shock

$\dot{m}_2$ measured inlet mass-flow rate

p pressure

p_t total pressure

R Reynolds number

ψ angle of yaw, degrees

δ boundary-layer total thickness

Subscripts:

2 conditions at diffuser exit

∞ conditions in free stream

δ based on boundary-layer total thickness

APPARATUS

Wind Tunnel

The investigation was made in the Langley 20-inch (50.8 cm) variable supersonic tunnel. Characteristics of this tunnel are given in reference 3. The test Mach number was 2.5, which corresponds to the local Mach number underneath the wing of a supersonic transport flying at a Mach number of 2.7 with an angle of attack of 4°. A total temperature of 70° F (21° C) and a total pressure of 125 psia (86.18 N/cm^2) gave a Reynolds number based on cowl diameter 5 inches (12.7 cm) of 10.8×10^6, which is very near that which an actual supersonic transport twin inlet with a 6.5 foot (1.98 meters) cowl diameter would encounter in flight at Mach 2.7 and an altitude of 65,000 feet (19,812 meters).

Model

The basic model consisted of a semicircular inlet which simulated one-half of a twin-inlet configuration and which was pylon-mounted to a plate simulating the wing. Photographs and drawings of the model are presented in figures 2 and 3. The inlet was mounted upside down from the actual flight configuration for convenience in handling. The plate simulating the wing was parallel to the free stream; thus, the model has no wing compression. Pressure probes were used in place of a second twin inlet and are discussed later.

The centerbody of the semicircular external-internal compression inlet was fixed at the design Mach number position and the internal contraction prohibited the inlet from starting throughout the investigation. Although this condition did not allow examination of the effects of the initial pulse which results when an external-internal compression inlet unstarts, the magnitude of this initial pulse is only slightly greater than the pulses of the unstarted inlet flow field which follows (unpublished industry data and ref. 1). Some detailed tailoring of the successful splitter plates may be necessary to isolate the first unstart shock. The half-cone centerbody has a 12.5° half-angle; the internal and external cowl lip angles of the inlet are 0° and 5°, respectively; and the inlet contraction ratio A_t/A_i is 0.52. All splitter plates provided 2.5° of compression, which reduced the local Mach number to 2.4, and the centerbody shock was directed toward the cowl lip at this design Mach number.

Photographs, composite sketches, and dimensional drawings of the various splitter plates investigated are shown in figures 4, 5, and 6. The only difference between plates 3 and 4 was that plate 3 had 0.375-inch (0.95-cm) extensions on its upper and lower edges. The very large plate, number 5, was used only in the special case of testing at zero mass flow. The three pylons, for which the distances from the cowl lip to the upper surface of the wing plate are one-half, one-fourth, and one-tenth the inlet diameter, are designated

the high, medium, and low pylons, respectively. The models can be yawed up to 6^{o}, with the inlet to the windward side, by shifting the pylon on the wing plate. Yawing the unstarted inlet to the windward side was believed to be the most critical test of the splitter-plate performance and therefore, no tests were made with the model yawed in the opposite direction.

The fixed wing plate was used to simulate the undersurface of the wing. It was necessary to simulate the wing because the shocks from the unstarted inlet might interact with the wing boundary layer and thereby allow disturbances to reach the opposite inlet. Since the interaction length is dependent on Reynolds number based on boundary-layer thickness R_{δ} (ref. 4), it was necessary to duplicate the value of R_{δ} expected on a supersonic transport. For a supersonic transport at 65,000 feet (19,812 meters) with a local Mach number under the wing of 2.5 and with a streamwise length of 45 feet (13.72 meters) from the leading edge to the inlet, the R_{δ} is 0.9×10^{6}. To obtain this value of R_{δ} with a smooth plate, the plate would have to extend 38 inches (96.5 cm) ahead of the inlet. A plate of this size was physically impractical for the Langley 20-inch (50.8-cm) variable supersonic tunnel. It was decided, therefore, to obtain the proper boundary-layer thickness by use of distributed roughness on a smaller 20-inch (50.8-cm) long wing plate. Number 120 carborundum, with a nominal height of 0.0049 inch (0.0124 cm), was distributed over the first 15 inches (38.1 cm). (The charts of ref. 5 were used in determining roughness height.) This arrangement allowed 4 to 5 inches (approximately 10 to 13 cm) on the surface of the plate after the distributed roughness region for the boundary layer to recover its normal shape before encountering any shocks. Measurement of the boundary-layer thickness in schlieren photographs taken during the investigation showed that δ was slightly less than 0.4 inch (1 cm) and corresponded to $R_{\delta} = 0.9 \times 10^{6}$, the desired Reynolds number.

Instrumentation

Pitot tubes were used in place of a second inlet to indicate whether disturbances reached the other side of the splitter plate. This procedure reduced the complexity of the model significantly as compared with a model with a startable second inlet, although a startable second inlet would have been advantageous in determining the effects of disturbances on inlet operation. Also, since the tunnel blockage area was reduced by elimination of the second inlet, a larger model could be used and full-scale Reynolds numbers were obtainable.

The three pressure gages which indicated whether disturbances reached the side of the splitter plate opposite the inlet were located inside the centerbody. This method of mounting minimized the pressure lag time by decreasing the length of pressure tubing necessary. The three probes were subjected to pitot pressures at positions which would

correspond to the two points where the cowl lip of a second twin inlet would join the splitter and at the midpoint between these two. They were positioned 0.3 inch (0.76 cm) from the splitter plate to eliminate any plate boundary-layer effects. (See fig. 3.) The pitot-pressure gages were originally 100 psia (69 N/cm^2) Statham gages but were changed to 300 psia (207 N/cm^2) Statham gages early in the investigation because the 100 psia (69 N/cm^2) gages could not withstand the severe fluctuating pressures which were encountered when flow disturbances reached the probes. A record of the output of these gages was taken continuously during each run on a direct readout oscillograph. The frequency response of the pressure-measuring system was determined with an audio-signal generator and loud speaker and was found to be approximately flat to at least 1000 cycles per second. The system was also found to have a weak resonant frequency of 280 cycles per second, which occasionally caused 280-cycle "noise" that is not the result of disturbances from the unstarted inlet reaching the probe.

Mass-flow plugs were used to control and determine the mass flow through the unstarted inlet. These plugs were semicircular aluminum blocks which have various sizes of nozzle-type holes to pass the flow. These holes were assumed to have a flow coefficient of 0.97 (ref. 6). The exit total pressure used in calculating the inlet mass flow was measured by a 100 psia (69 N/cm^2) Statham gage connected to a single total-pressure probe in the diffuser exit.

Flow Visualization

In order to aid in the evaluation of the effectiveness of the splitter plates, both schlieren and shadowgraph movies were obtained. Schlierens were taken with a 35-millimeter camera at 50 frames per second and show all the flow except that which was blocked from view by the splitter plates.

A unique shadowgraph method was used to obtain motion pictures of the flow field on the splitter plates. This method consisted of reflecting parallel light off the splitter plates (which are polished stainless steel to give a mirror finish), passing the reflected light through an achromatic convex lens, and focusing the light into a 16-millimeter high-speed motion-picture camera, operating at 2000 frames/sec. (See fig. 7.) The camera pictured the shadowgraph image at the point at which the camera lens was focused. Flow separations and shocks on the splitter plates may be seen clearly on the shadowgraphs since light rays are deflected by these flow disturbances. The sensitivity of the shadowgraphs to flow disturbances could be adjusted by changing the camera lens focus setting. (For example, by focusing the camera at the distance to the splitter plate, the sensitivity was greatly reduced and no disturbances could be seen, but by focusing at distances closer to the camera, much greater sensitivity was obtained.) The edges of the shadowgraphs were of poor quality because the splitter-plate edges were rounded slightly in the polishing process.

TESTS

The tests were made by obtaining the highest total pressure possible in the tunnel, approximately 125 psia (86 N/cm^2), and then taking shadowgraph or schlieren pictures. For each configuration, shadowgraphs and schlierens were taken during separate but virtually identical test runs. While the pictures were being taken, the speed of the direct readout oscillograph, which continuously recorded the pitot pressures, was changed from 5 in./sec (12.7 cm/sec) to 25 in./sec (63.5 cm/sec).

The pitot-pressure recordings were used to determine splitter-plate effectiveness. The conservative criterion used was that a splitter plate was considered to be ineffective if the recorded pitot pressures indicated any disturbances whatsoever. A flow disturbance reaching the pitot probes could be expected to cause fluctuating pitot pressures and/or a change in the level of the pitot pressure. In order to determine whether any change in pitot-pressure level occurred during this investigation, a number of configurations were tested both with and without the inlet cowl. The no-cowl configuration simulated a started inlet in that there was no normal shock on the inlet side of the splitter plate and no disturbances could possibly reach the pitot tubes. The pitot pressures were always identical for the tests on the cowl and no-cowl configurations; therefore, no changes in pressure level alone occurred. Thus, during this investigation, flow disturbances which reached the pitot tubes caused fluctuations in the pitot pressures.

Tests were conducted with an "open" diffuser exit and with reduced mass flow; in both cases, mass-flow control plugs were used to determine mass-flow ratio. For the inlet model, the mass-flow ratio $\dot{m}_2/\dot{m}_1$ is defined as the ratio of the mass flow passing through the inlet to that passing through a stream tube of area A_i and located behind the splitter-plate shock. The tunnel conditions, exit total pressure, and the area and flow coefficient of the nozzle determine the mass-flow ratio. A mass-flow ratio of 0.72 for the "open" diffuser exit condition was found by use of a mass-flow plug which choked the exit (as seen by a large increase in exit p_t) but caused no change in the inlet flow field (as shown by the shadowgraphs) when compared with tests when no mass-flow plug was used. For this case, therefore, the exit is just choked, and the mass-flow ratio is the same as if no plug had been used.

With the diffuser exit open, a complete series of tests were conducted at the various pylon heights and angles of yaw. Open-exit condition tests were considered the most significant for the following reason. There are numerous causes of inlet unstarts, and the mass flow through an unstarted inlet normally depends on exactly the type of unstart that has occurred. However, future supersonic inlets should incorporate subsonic bypass doors which, although they may not be able to eliminate inlet unstarts completely, will react very rapidly (ref. 7). These bypass doors will pass any excess mass flow entering

the unstarted inlet which cannot pass through the engine, as may be the case in certain types of unstarts. Thus, the unstarted inlet mass-flow ratio will depend only on the amount of internal contraction that the inlet has, and results with the diffuser exit open may be considered to simulate actual unstart conditions accurately. It should be remembered, however, that the initial pulse of the unstart is not simulated and that this pulse may require slight modifications to splitter plates which are successful for the open diffuser exit case. A limited number of reduced mass-flow tests were conducted which serve to indicate the performance of the splitter plates in the event that the subsonic bypass doors fail to open or do not react rapidly enough to prevent reduced mass flow in the unstarted inlet.

RESULTS AND DISCUSSION

Inlet Flow Field for the Open Diffuser Exit Case

An understanding of the flow field about the model is necessary to explain satisfactorily why a particular splitter plate did or did not isolate the unstarted inlet. The most important characteristic of the unstarted inlet flow field was that it was steady for the open-exit condition. This characteristic demonstrates that this particular inlet had some degree of subcritical stability. A schematic drawing is shown in figure 8 which is representative of the unstarted steady inlet flow field in that the flow always maintained this basic structure, regardless of the splitter plate, pylon height, or angle of yaw. This basic inlet flow field consisted of a cone separation, with the accompanying separation shock, followed by a normal shock in front of the inlet cowl. The normal shock assumed a bifurcated structure, although it is sometimes difficult to discern this structure.

There were also two "ridge" lines. The ridge line, where the plate boundary-layer flow has been deflected outward away from the cone, is a phenomenon of the glancing interaction of a shock wave with a turbulent boundary layer and is caused by upstream pressure influences of the separation shock in the splitter-plate boundary layer. (The Reynolds number based on the distance from the splitter-plate leading edge to the interaction region was always greater than 5×10^6; therefore, the boundary layer should be turbulent in all cases.) Tests using oil flow indicated that the plate boundary layer flowed in the direction shown in figure 8, the boundary layer behind the upper ridge line flowing upward toward the upper ridge line and the boundary layer behind the lower ridge line flowing downward and toward the lower ridge line. (See refs. 8 and 9 for a discussion of glancing-shock—turbulent-boundary-layer interaction.) On the upper and lower edges of the splitter plate, a disturbance and an accompanying shock can be seen which occurred where the ridge line reached the splitter-plate edge. The outflow in the boundary layer along and behind the ridge line is believed to have caused this disturbance. Figure 9 is a composite photograph, made up of a schlieren showing all the flow except

that blocked from view by the splitter plate and a shadowgraph picturing the flow on the splitter plate. For clarity, the outline of the model has been marked. This photograph shows a typical flow field about the complete model, and various disturbances are pointed out in the figure. Wires, called dimension wires, were placed outside the tunnel for many of the tests and were positioned 1 inch (2.54 cm) apart. They were used to provide a known distance on the photographs and in this manner aided in reducing the shadowgraphs and schlierens to the size necessary to form a composite photograph. The shocks reflected from the tunnel floor were shocks from supporting struts and the wing leading edge. None of these shocks affected the pitot pressures at any time.

The preceding interpretation of the inlet flow field was verified by tests conducted without a splitter plate at Mach 2.4. Although the splitter plate was removed, the cowl was still completely enclosed and, as before, the inlet did not start. The flow field which results is shown in figure 10 and it is seen that despite the pressure-relieving effects which occur without the splitter plate, the flow field was essentially the same as the flow when the splitter plate was present. Comparisons show very little change in the position of the cone separation and accompanying shock. When the structure of the model flow field is known, the schlieren and shadowgraph pictures can be used to explain the splitter-plate performance as determined from the pitot-pressure traces.

Splitter-Plate Effectiveness for the Open Diffuser Exit Case

As stated previously, the open-exit configuration should best simulate an actual inlet unstart which occurs while fast-acting subsonic bypass doors are in operation. Results with the high pylon and open diffuser exit are presented first. Figures 9, 11(a), 11(b), and 11(c) show the inlet flow fields for splitter plates 1, 2, 3, and 4, respectively, and the corresponding pressure traces are presented in figures 12(a), 12(b), 12(c), and 12(d). Figures 9, 11(a), 11(b), 12(a), 12(b), and 12(c) show that for splitter plates 1, 2, and 3, all the flow fields are very similar and all the pressure traces for these plates are steady. (The particular levels of the three traces are very slightly different for the various splitter plates because of slight differences in the back side of the splitter plates opposite the inlet. These differences were necessary to maintain a constant 2.5° angle to the free stream on the inlet side of all the splitter plates.) Thus, all three plates are effective in isolating the unstarted inlet at the high pylon height, even though plates 2 and 3 are somewhat smaller than splitter plate 1.

Since the shadowgraph pictures show that the shock structure ahead of the inlet did not reach the tip of the conical centerbody and plate 2 was successful without extending beyond this point, these tests indicate that it is not necessary for a plate to extend beyond the centerbody tip to be successful.

When splitter plate 4 was used with the high pylon, the results shown in figure 12(d) indicate that the inlet flow field was not isolated. Although the flow field of the unstarted inlet (fig. 11(c)) appears to be the same as in the previous photographs for plates 1, 2, and 3, the upper and lower pitot-pressure probes were being disturbed. The pressure-relieving effects at the edges of the splitter plates tend to allow disturbances to flow around the edges of the plates, and evidently the disturbances negotiated the turn on splitter plate 4 and reached the pitot-pressure probes because the upper and lower edges of plate 4 did not extend past the cowl lip. It is apparent that some extension is necessary and it has already been shown that splitter plate 3 with its 0.375-inch (0.95-cm, 7.5-percent inlet cowl diameter) extensions (fig. 6) is successful in preventing the unstarted flow field from spilling around the upper and lower edges.

Splitter plates 1, 2, and 3, which were successful at the high pylon height, were also tested at the medium pylon height of 1/4 D. (See figs. 13 and 14.) In all instances, the pressure traces were identical to the steady traces at the high pylon height; thus, all three plates were again successful in isolating the unstarted flow field. This condition occurred despite the reduction in pylon height and the consequent stronger interaction with the wing-plate boundary layer, as seen in figure 13.

The three plates were next tested at the low pylon height of 1/10 D. (See figs. 15 and 16.) Very strong interactions with the wing-plate boundary layer can be seen in figure 15. The pressure traces in figure 16 show that the lower probe was always disturbed; however, for plates 1 and 2 the disturbances resulted from the interference of the wing-plate boundary layer with the probe and not from disturbances emanating from the unstarted inlet. This result was determined from tests of the same configurations without an inlet cowl which resulted in identical pressure disturbances on the lower probe. The bottom of this probe was 1/2 inch (1.27 cm) from the wing-plate surface, whereas the boundary layer was about 0.4-inch (1-cm) thick, and the normal shock in front of the probe undoubtedly interacted with the wing-plate boundary layer to cause these slight disturbances. Thus, plates 1 and 2 were successful in isolating the inlet flow field and the strong inlet interaction with the wing-plate boundary layer. It is significant that both of these effective plates have lower edges which lie on the surface of the wing.

Splitter plate 3, however, leaves a gap of 0.125 inch (0.32 cm) between the lower edges of the splitter plate and the surface of the wing plate at the low pylon height. When plate 3 was tested with this pylon, the disturbances on the lower pressure probe (fig. 16(c)) were considerably greater than the disturbances due to the wing-plate boundary layer alone. Here, the inlet-flow-field wing-boundary-layer interaction propagated through the gap to disturb the lower probe, and therefore, splitter plate 3 was ineffective at the low pylon height. Thus, in order to isolate twin inlets at low pylon heights, it

becomes necessary to have the splitter plate and wing connect. On an actual practical configuration, such an arrangement would also be desirable for structural reasons.

The effects of yaw with the diffuser exit open were also investigated. Plates 1, 2, and 3 were tested at all three pylon heights at the maximum test angle of yaw of 6° with the inlet windward. Figure 17 shows typical results. The normal shock was moved farther forward of the inlet cowl, and the mass-flow ratio was reduced to approximately 0.62. The mass flow through the inlet capture area $\dot{m}_1$ is considerably higher at $\psi = 6^{\circ}$ than at $\psi = 0^{\circ}$, because the mass flow per unit area behind the splitter-plate shock is greater (by 27 percent) at $\psi = 6^{\circ}$ than at $\psi = 0^{\circ}$. Thus, although the inlet mass flow $\dot{m}_2$ was increased, the mass-flow ratio $\dot{m}_2/\dot{m}_1$ was reduced for $\psi = 6^{\circ}$. Although adverse effects might have been expected, in no case was the ability of the splitter plates to isolate the unstarted inlet altered by a yaw of 6°.

Splitter-Plate Effectiveness for the Reduced-Mass-Flow Case

A limited number of tests were conducted in which the mass-flow ratio was reduced below 0.72 (open-exit condition). Photographs of the general sequence when splitter plate 1 was tested at reduced mass flows is shown in figures 18 and 19. The numbers on the figures correspond to frame numbers of the motion pictures. As the mass flow was reduced below 0.72, buzz of high frequency began at a value of $\dot{m}_2/\dot{m}_1$ of about 0.65. With further mass-flow reduction, the buzz changed to a lower frequency oscillation of larger amplitude and the high-frequency mode was superimposed on this oscillation. The buzz became more severe as the mass flow was reduced still further. When plate 1 first failed (that is, became ineffective) at $\dot{m}_2/\dot{m}_1 = 0.57$, the upper and lower pitot pressures were disturbed. With lower mass flows, the probe disturbances were more severe and at zero mass flow, all three probes were disturbed. The inlet buzz was so strong at zero mass flow that even the largest splitter plate, number 5, was unable to isolate any of the probes from disturbances.

It was found that this general sequence of events occurred with reduced mass flow for splitter plates 1 and 3 at all pylon heights and for angles of yaw of 0° and 6°. (Plate 2 results are discussed later.) Figure 20(a) presents the performance of splitter plates 1 and 3 for various mass flows and $\psi = 0^{\circ}$. Each point shown was usually the average value of points, very near each other, obtained in separate tests on the same configuration (shadowgraph and schlieren tests). Points where the splitter plates were ineffective are denoted by flagged symbols. From this figure, it is seen that for $\psi = 0^{\circ}$, at the upper two pylon heights (open symbols), plates 1 and 3 are successful in isolating the unstarted inlet down to a mass-flow ratio of about 0.65 but fail when the ratio is reduced to 0.57. Use of the low pylon height (solid symbols) at $\psi = 0^{\circ}$ shifted the mass-flow ratio pressure-recovery curve only slightly from that for the high and medium

pylon results. Plate 1 at the low pylon height fails at $\dot{m}_2/\dot{m}_1 = 0.55$ (about the same value as for the two higher pylons) but plate 3 is, of course, never successful at the low pylon height because of the gap between the splitter plate and the wing surface.

The performance and inlet-flow-field characteristics of splitter plate 2 at $\psi = 0^\circ$, shown in figure 20(b), were the same as those for splitter plate 1 down to the mass-flow ratio of 0.64. As the mass flow was further reduced to 0.57 (the mass-flow ratio at which splitter plate 1 failed), plate 2 became ineffective at the medium pylon height, where the lower pitot tube was disturbed, but was still effective at the high and low pylon heights. When an attempt was made to reduce the mass flow further, the flow completely changed character to a steady separated condition and the mass-flow ratio dropped to 0.27. This condition is shown by the shadowgraphs in figure 20(b). Since the separation occurred at one of the corners on the front of the plate, it appears that the separation may have been induced by slight pressure gradients caused by the conical flow fields that the corners generate. By choking the flow still further, $\dot{m}_2/\dot{m}_1$ became 0.19. At this condition the flow still remained separated, but the lower probe was disturbed. The question of whether plate 2 was successful between a mass-flow ratio of 0.57 and 0.27 cannot be determined because mass-flow ratios in this range were unattainable, but at best, any success was marginal inasmuch as ineffectiveness of the plate was already indicated for the medium pylon height at $\dot{m}_2/\dot{m}_1 = 0.57$.

Some reduced mass-flow tests were also conducted at $\psi = 6^\circ$, and results are shown in figure 21. Plate 1 was successful at $\dot{m}_2/\dot{m}_1 = 0.57$, but failed at $\dot{m}_2/\dot{m}_1 = 0.5$. Plate 2 was successful at a mass-flow ratio of 0.54 but failed at 0.47. No steady separation occurred in the range tested (down to 0.47). Plate 3 was only successful for the open-exit condition $\dot{m}_2/\dot{m}_1 = 0.62$, but failed at $\dot{m}_2/\dot{m}_1 = 0.57$. Plate 3 probably fails somewhat earlier than plates 1 and 2 because its upper and lower edges extend only 0.075 cowl diameters as compared with 0.10 cowl diameters for plates 1 and 2.

The most important conclusion to be drawn from the tests with reduced mass flow is that reasonably sized splitter plates will continue to isolate an unstarted inlet at least down to a mass-flow ratio of approximately 0.65.

CONCLUSIONS

An investigation was made at a Mach number of 2.5 and a Reynolds number based on cowl diameter of 10.8×10^6 (approximately full-scale flight conditions for a supersonic transport) to determine the ability of various splitter plates to isolate an unstarted twin inlet. The investigation led to the following conclusions:

1. Splitter plates of practical size can isolate the unstarted twin inlet, at least as long as the mass-flow ratio is maintained above approximately 0.65.

2. It is necessary for the upper and lower edges of successful splitter plates to extend above and below the cowl lip. (An extension of 7.5 percent of the cowl diameter was successful.) It is not necessary, however, for the splitter plate to extend beyond the tip of the conical centerbody. The splitter plate should be tailored to fit the specific application required.

3. Splitter plates of reasonable size are successful for yaw up to 6^{o} with the unstarted inlet windward.

4. Pylon height has little effect except that at low heights where it is necessary that there be no gap between the splitter plate and the wing.

Langley Research Center,
National Aeronautics and Space Administration,
Langley Station, Hampton, Va., January 5, 1966.

REFERENCES

1. Motycka, D. L.; and Murphy, J. B.: Experimental Investigation of Inlet-to-Inlet Shock Interference. [Preprint] 650197, Soc. Automotive Engrs., Apr. 1965.

2. Robins, A. Warner; and Whitcomb, Richard T.: Additional Configuration Approaches. Proceedings of NASA Conference On Supersonic-Transport Feasibility Studies and Supporting Research. NASA TM X-905, 1963, pp. 277-290.

3. McRee, Donald I.; Peterson, John B., Jr.; and Braslow, Albert L.: Effect of Air Injection Through a Porous Surface and Through Slots on Turbulent Skin Friction at Mach 3. NASA TN D-2427, 1964.

4. Hammitt, Andrew G.; and Hight, Sylvester: Scale Effects in Turbulent Shock Wave Boundary-Layer Interactions. Proc. Sixth Annual Conference on Fluid Mechanics (Austin, Texas), Sept. 1959.

5. Clutter, Darwin W.: Charts for Determining Skin-Friction Coefficient on Smooth and on Rough Flat Plates at Mach Numbers Up to 5.0 With and Without Heat Transfer. Rept. No. ES 29074, Douglas Aircraft Co., Inc., Apr. 15, 1959.

6. Soundranayagam, S.: An Investigation Into the Performance of Two ISA Metering Nozzles of Finite and Zero Area Ratio. Trans. ASME, Ser. D: J. Basic Eng., vol. 87, no. 2, June 1965, pp. 529-532.

7. Kepler, C. Edward; and Barry, Frank W.: Engine Air Inlet Compatibility for the Supersonic Transport. [Preprint] 650225, Soc. Automotive Engrs., Apr. 1965.

8. Landrum, Emma Jean: A Study at a Mach Number of 2.01 of the Shock Boundary-Layer Interaction Resulting From the Deflection of a Wedge Mounted on a Bypass Plate. M. A. Thesis, The College of William and Mary, 1961.

9. Stanbrook, A.: An Experimental Study of the Glancing Interaction Between a Shock Wave and a Turbulent Boundary Layer. Tech. Note Aero. 2701, British R.A.E., July 1960.

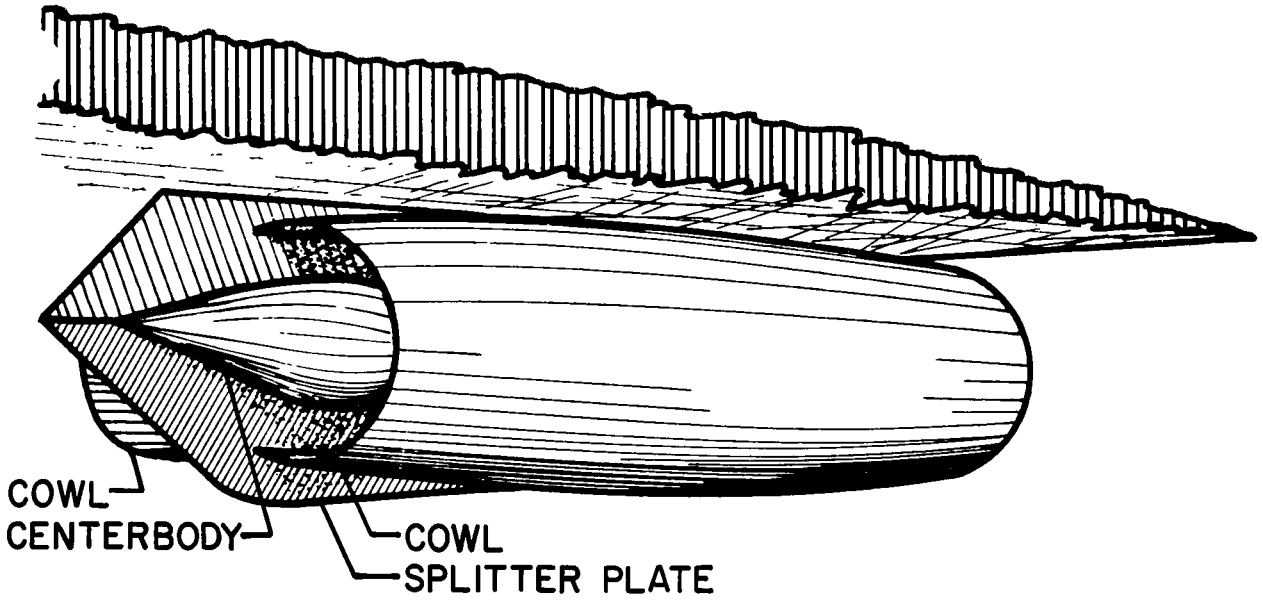

Figure 1.- Twin-inlet configuration.

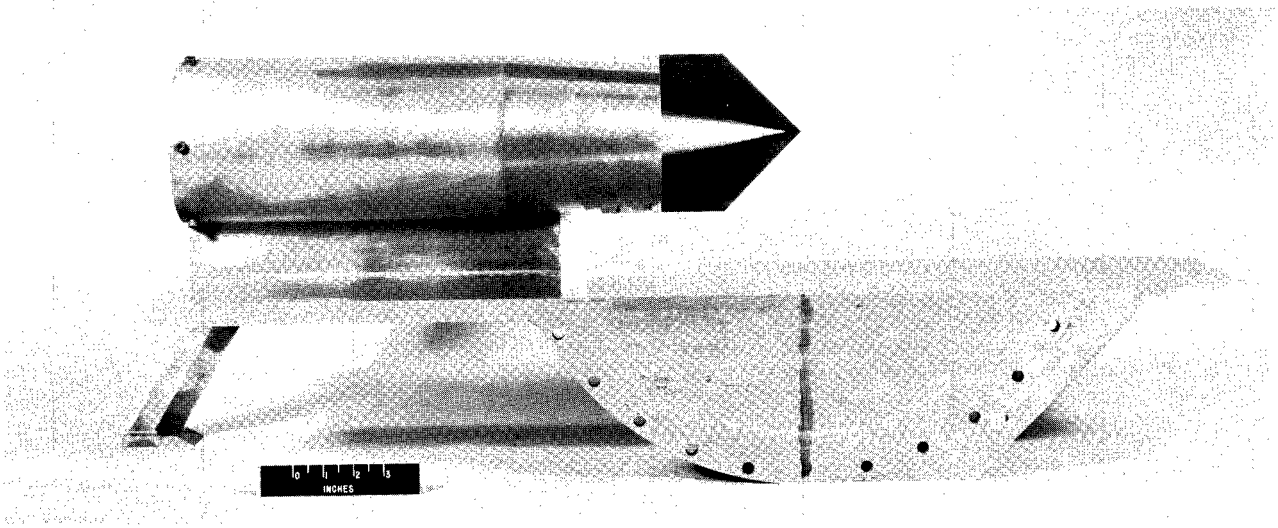

(a) Right side view.

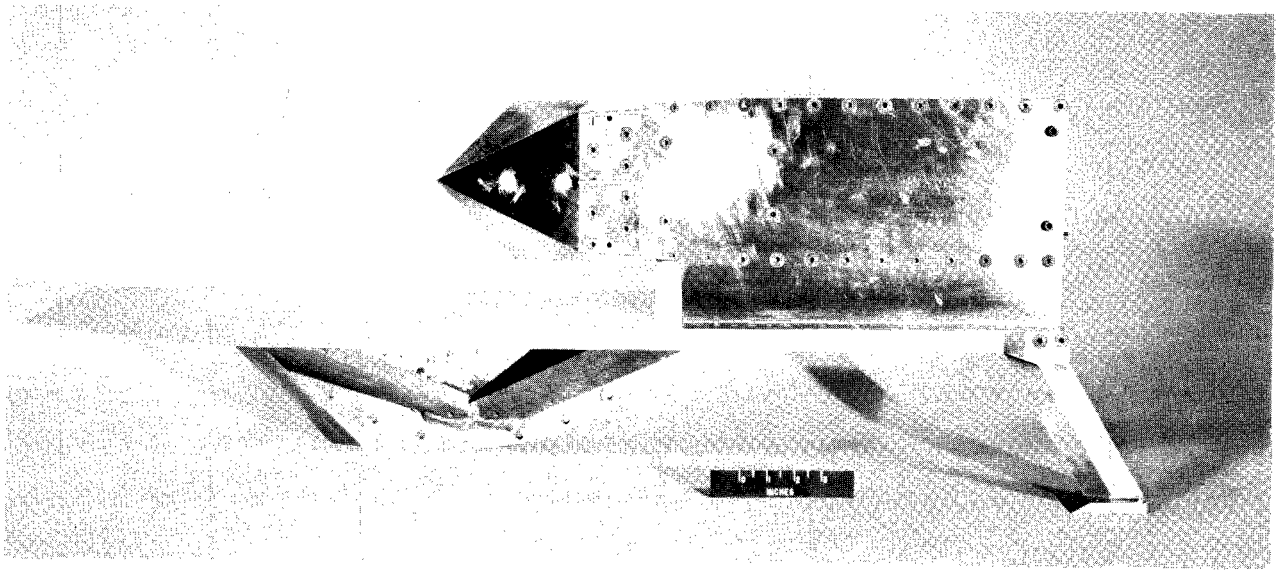

(b) Left side view.

L-66-1019

Figure 2.- Wind-tunnel model.

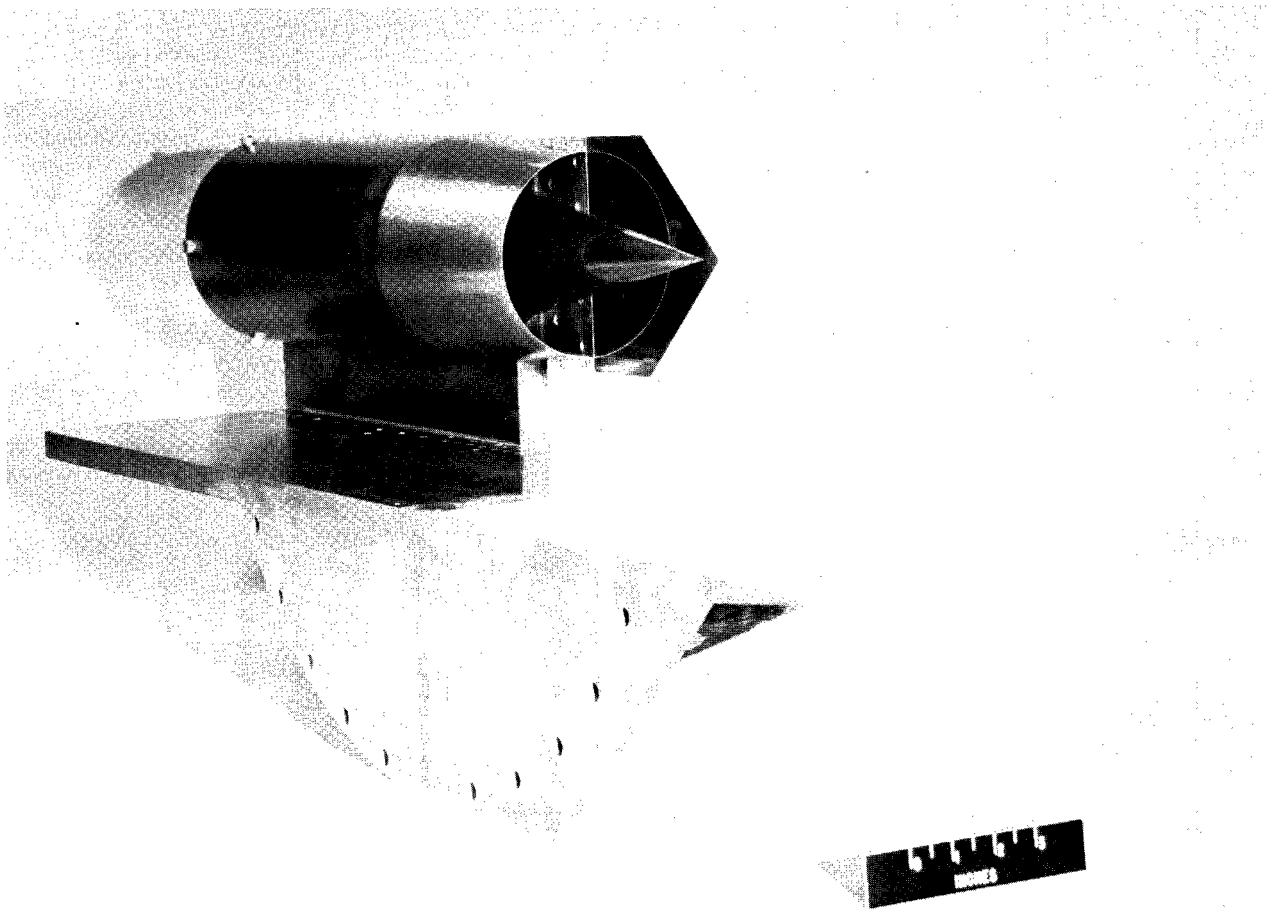

(c) Oblique view. L-64-3945

Figure 2.- Concluded.

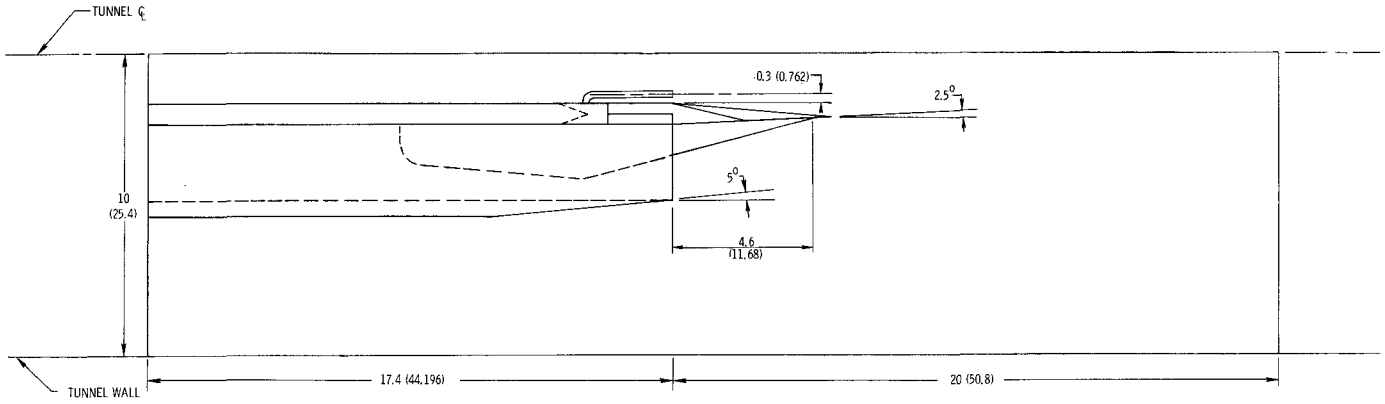

(a) Top view.

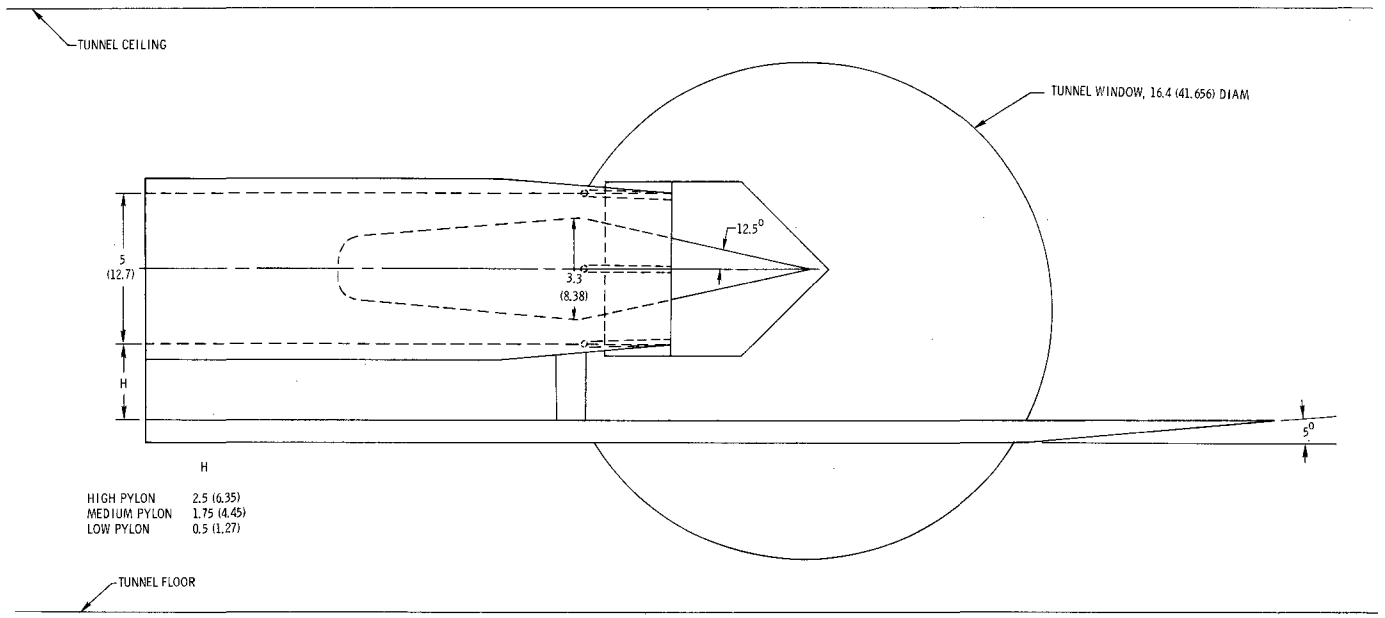

(b) Right side view.

Figure 3.- Drawings of wind-tunnel model. All dimensions are in inches (dimensions in parenthesis are in centimeters).

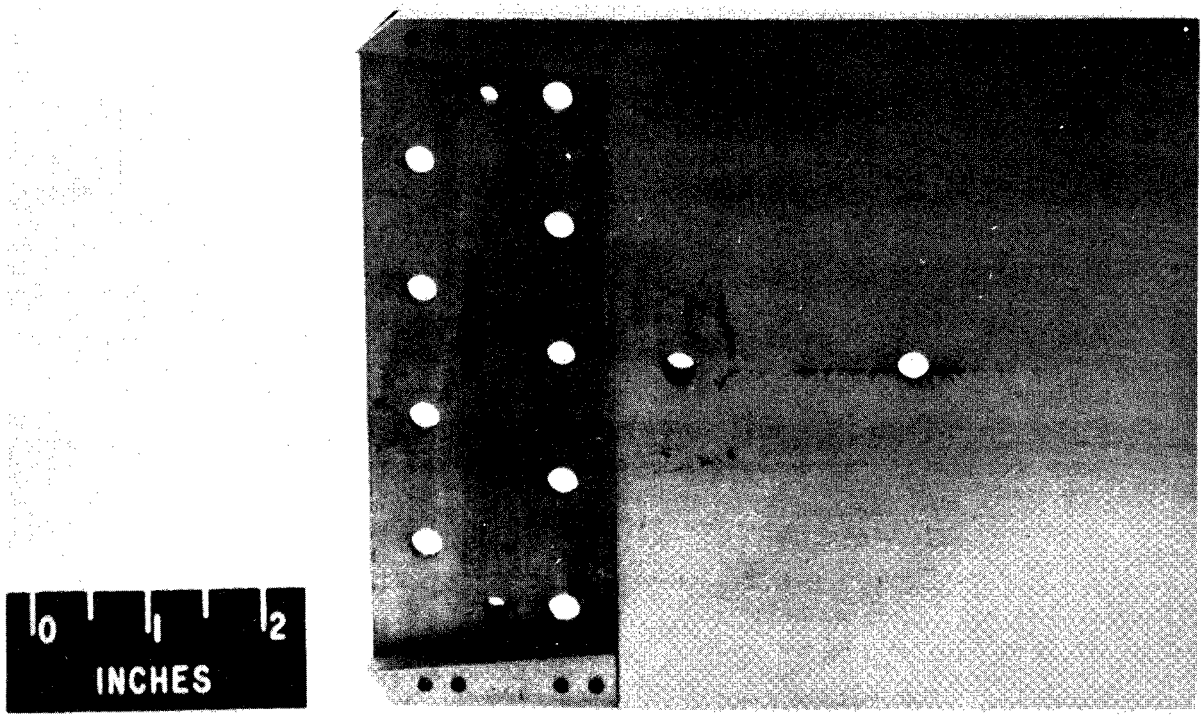

(a) Splitter plate 1.

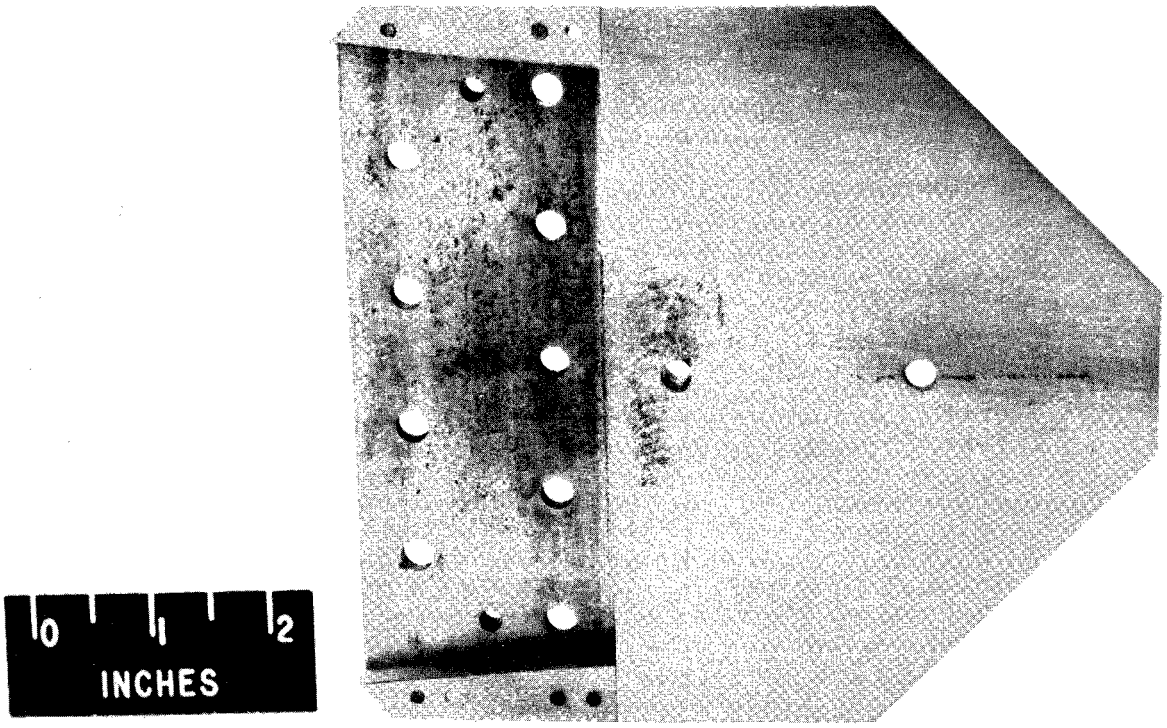

(b) Splitter plate 2.

Figure 4.- Splitter plates. L-66-1020

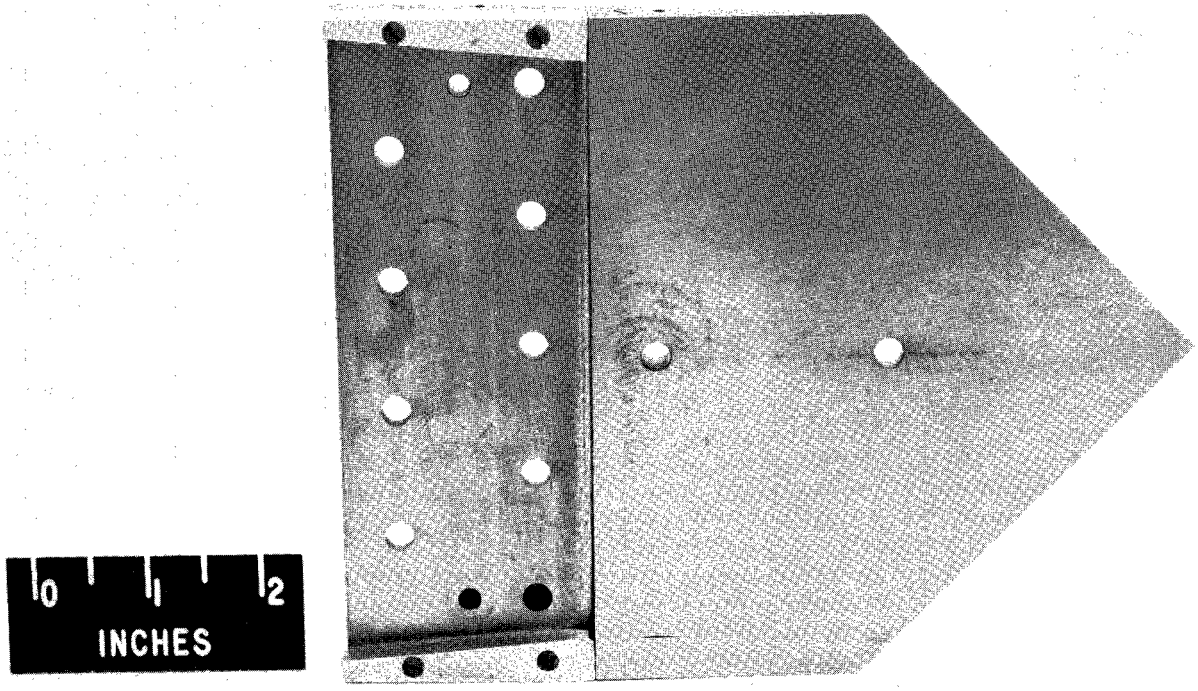

(c) Splitter plate 3.

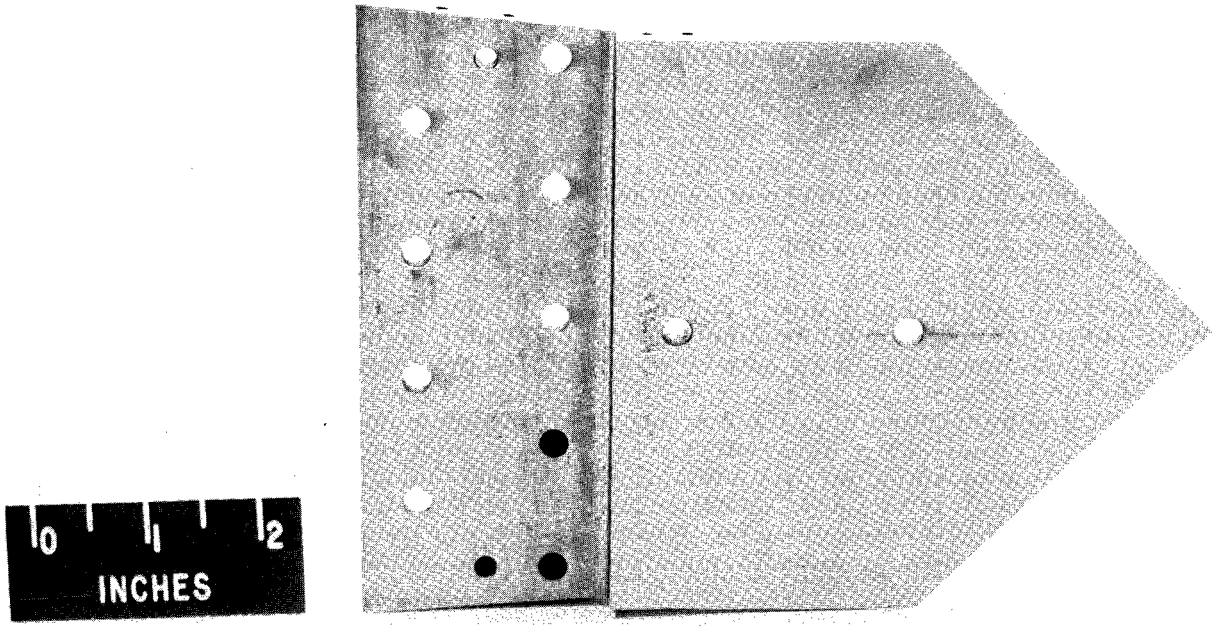

(d) Splitter plate 4. L-66-1021

Figure 4.- Continued.

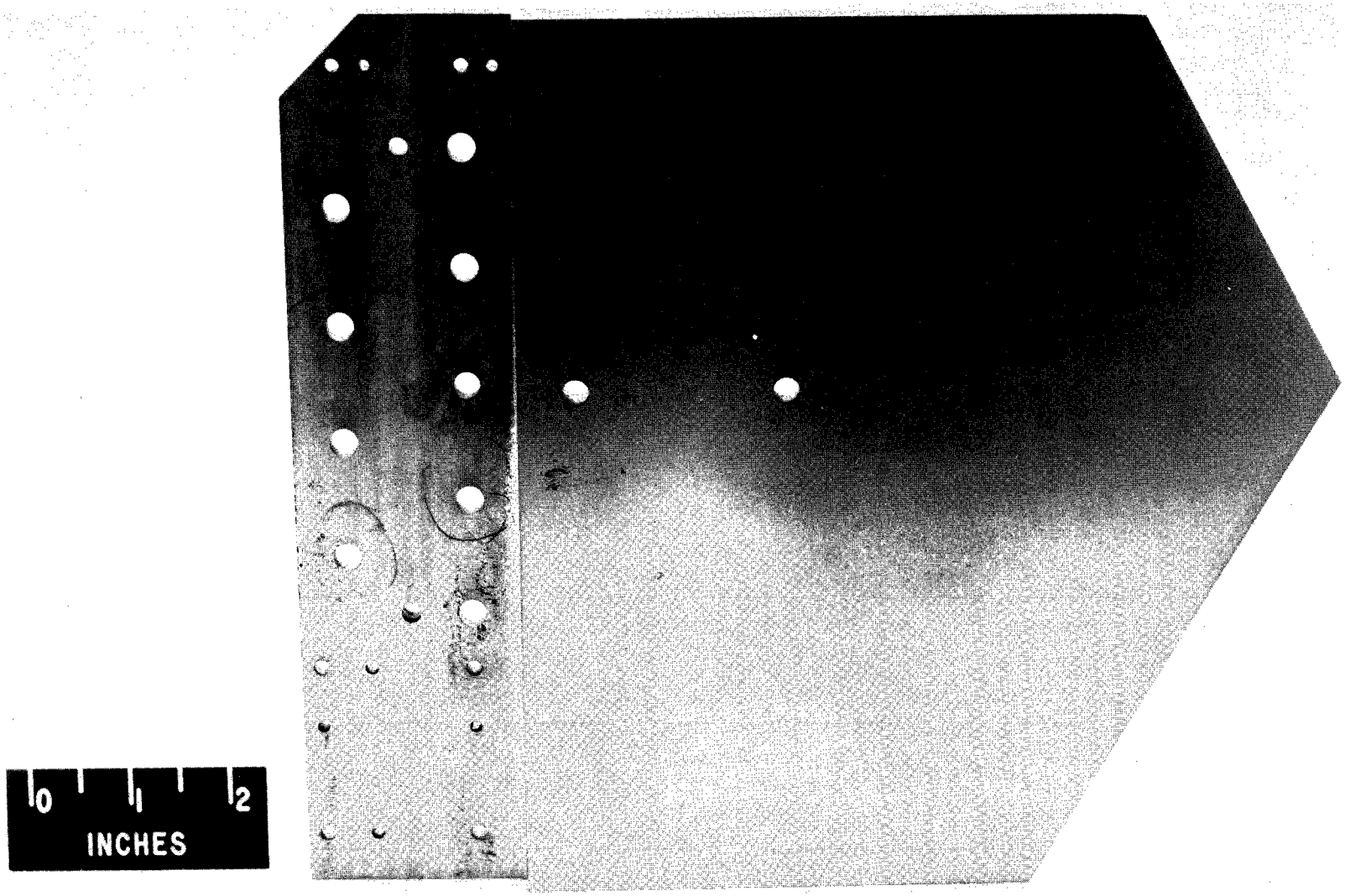

(e) Splitter plate 5. L-66-1022

Figure 4.- Concluded.

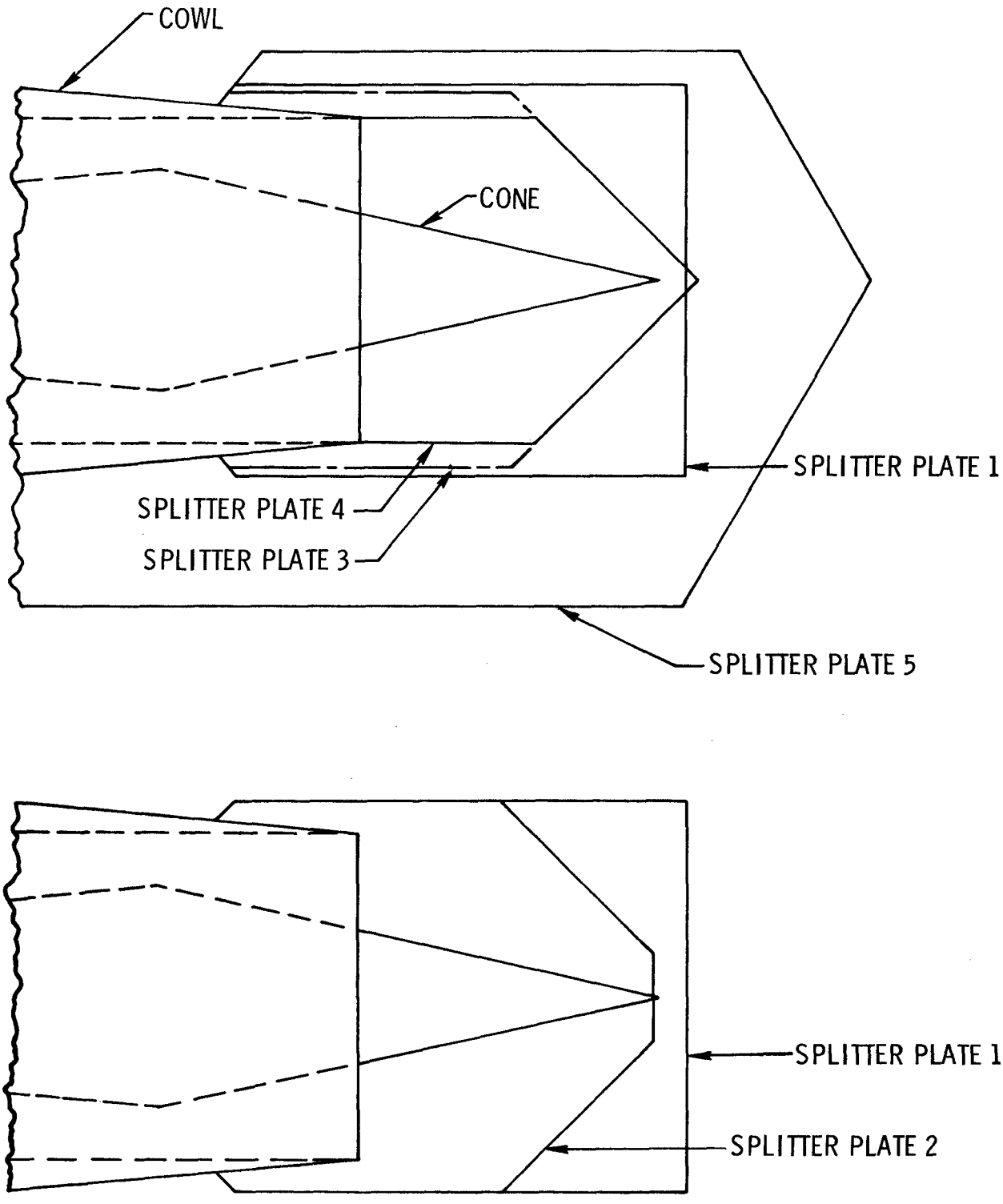

Figure 5.- Composite drawings of mounted splitter plates.

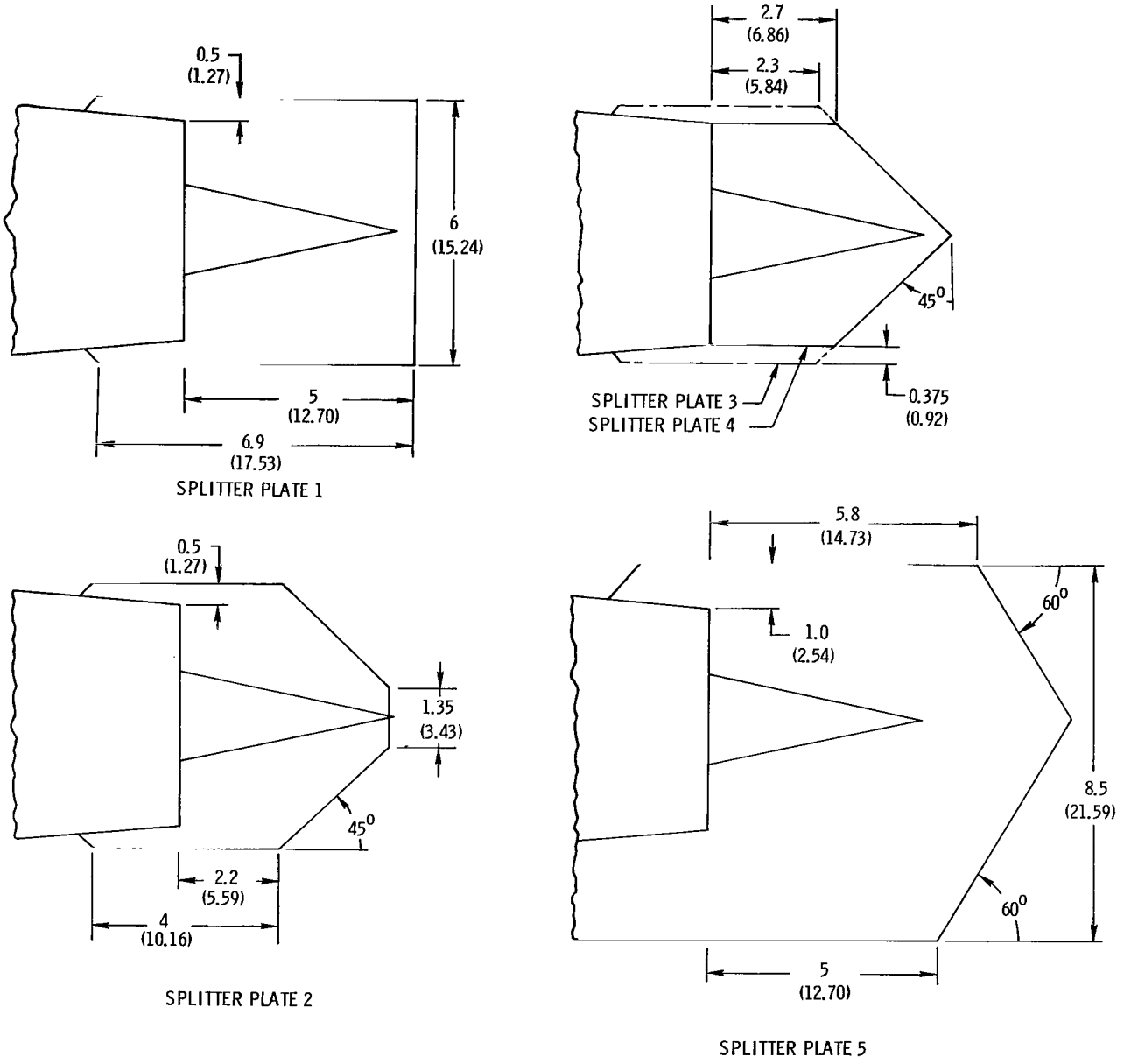

Figure 6.- Dimensional drawings of mounted splitter plates. All dimensions are in inches (dimensions in parenthesis are in centimeters).

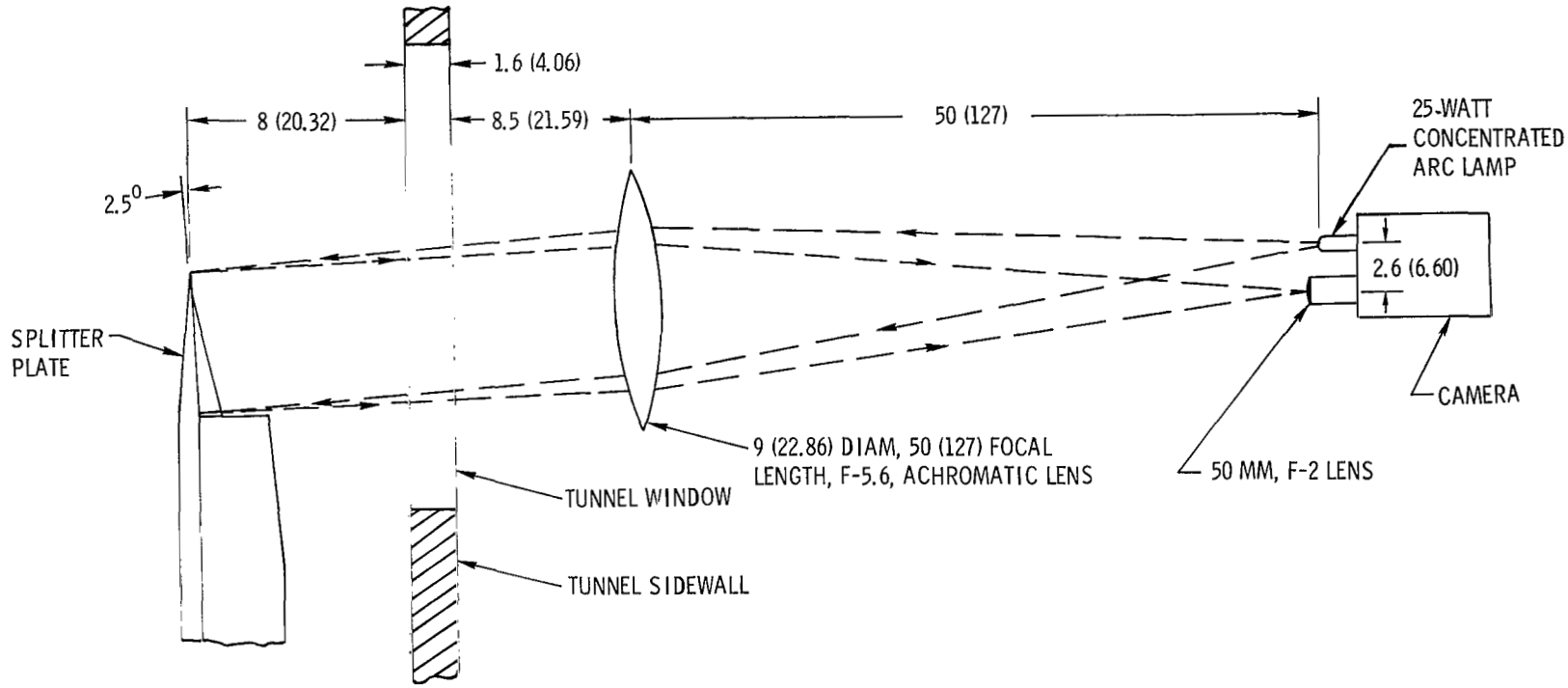

Figure 7.- Schematic drawing of shadowgraph system. All dimensions are in inches (dimensions in parenthesis are in centimeters).

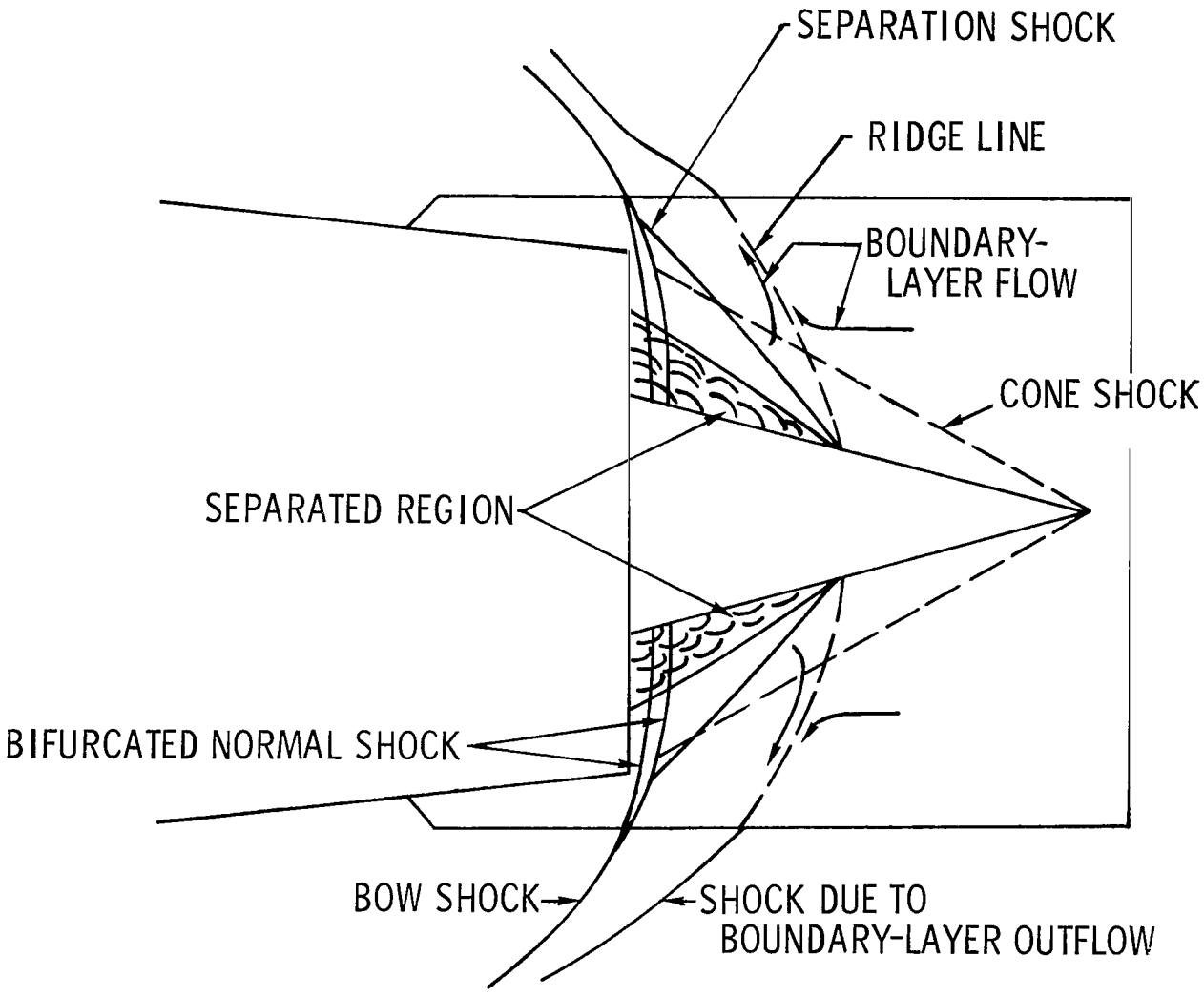

Figure 8.- Sketch of typical inlet-flow field.

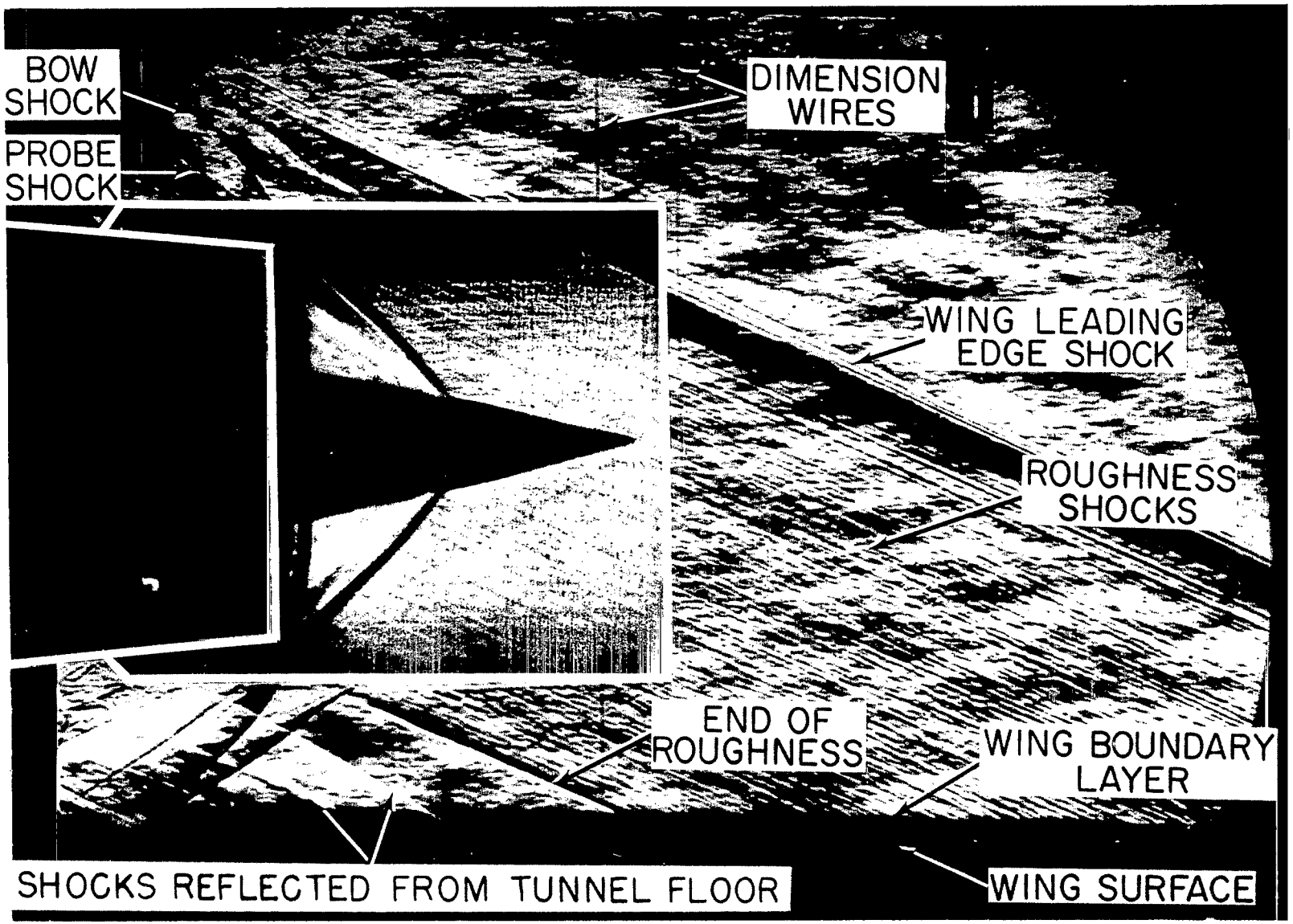

Figure 9.- Composite shadowgraph and schlieren of the flow. Splitter plate 1; high pylon; $\psi = 0^0$; $\dot{m}_2/\dot{m}_1 = 0.72$. L-66-1003

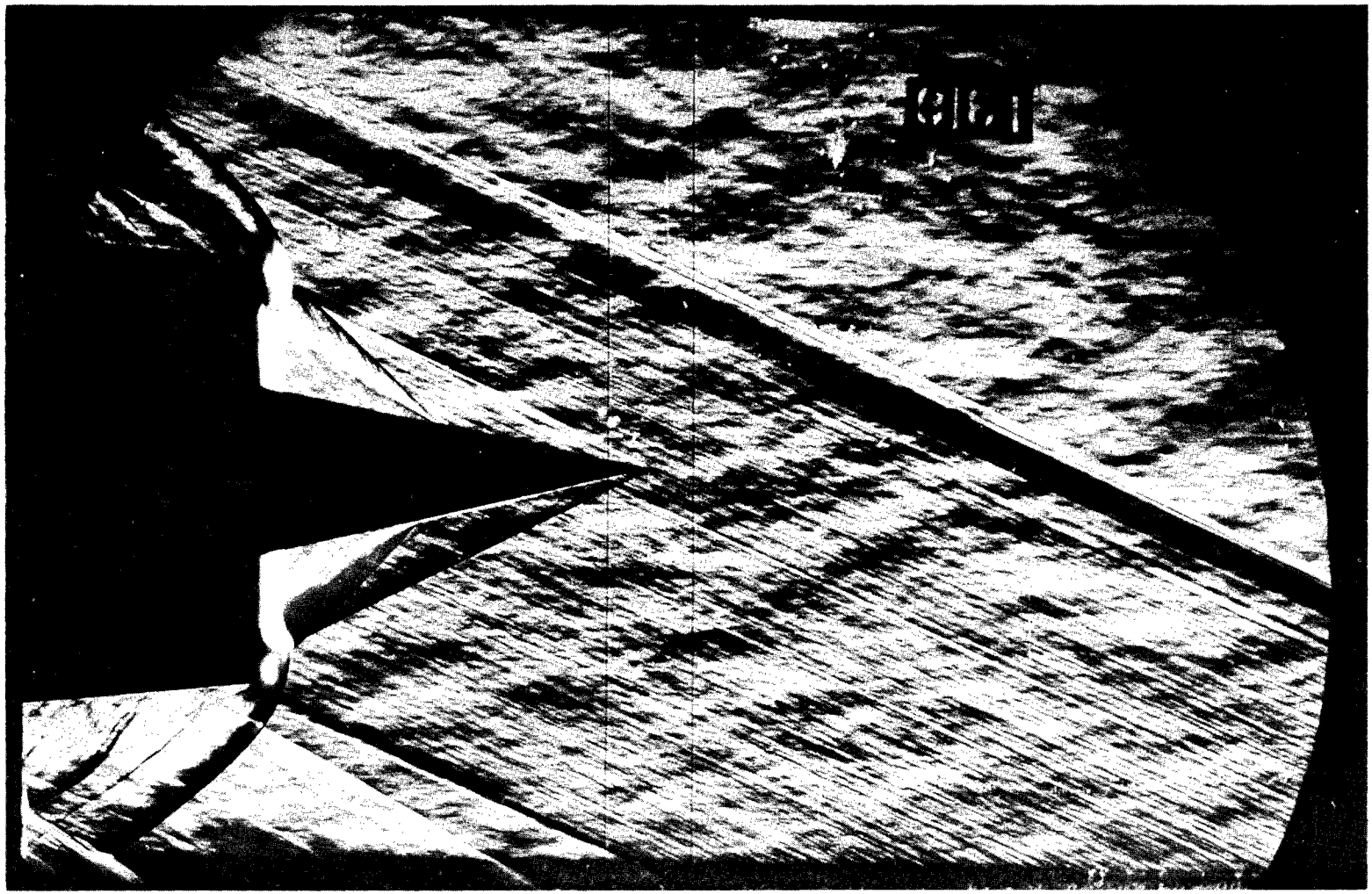

Figure 10.- Schlieren of flow occurring with no splitter plate. High pylon; $\psi = 0^{0}$.

L-66-1004

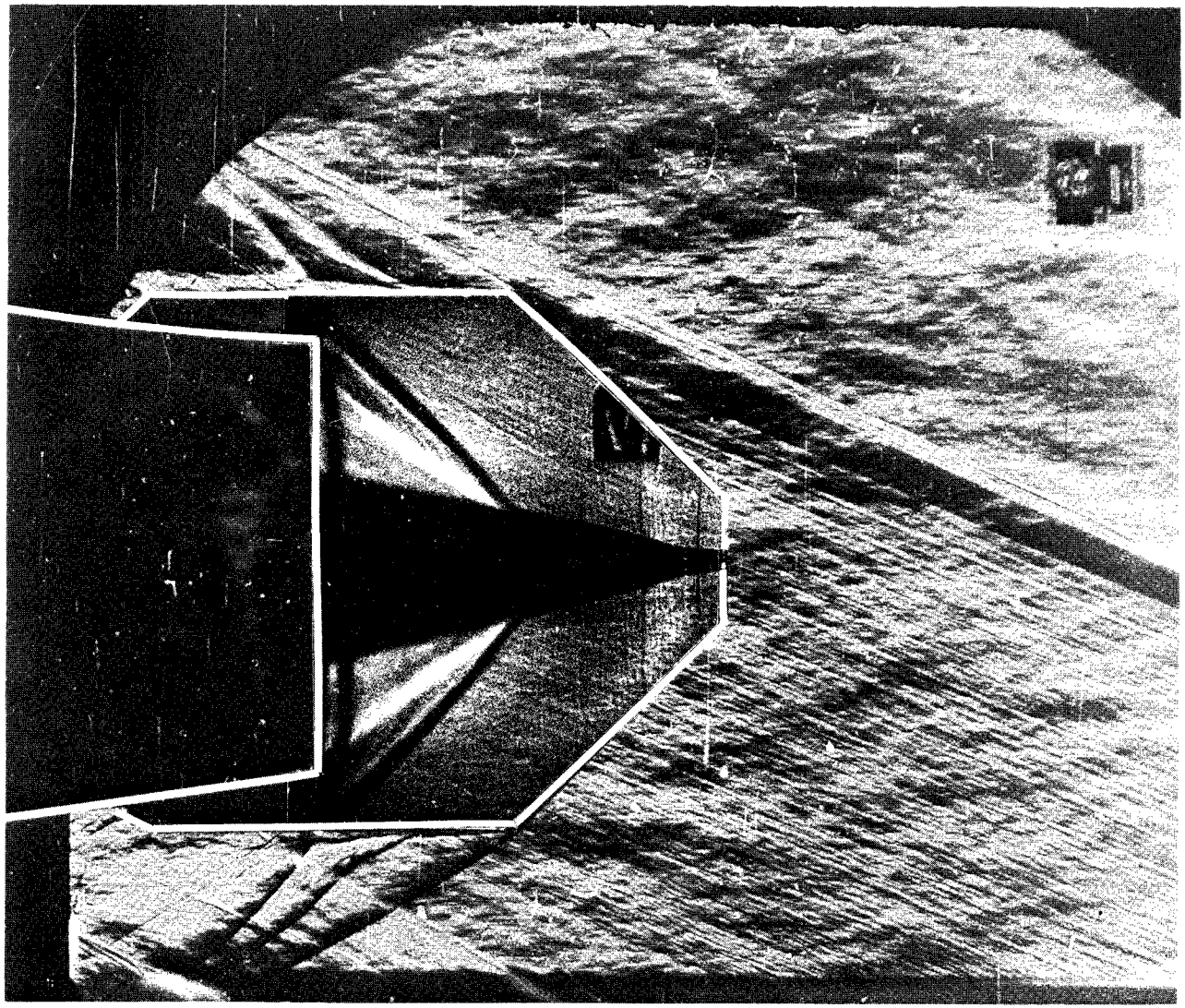

(a) Splitter plate 2.

Figure 11.- Composite shadowgraph and schlieren of the flow. High pylon; $\psi = 0^{o}$; $\dot{m}_2/\dot{m}_1 = 0.72$.

L-66-1005

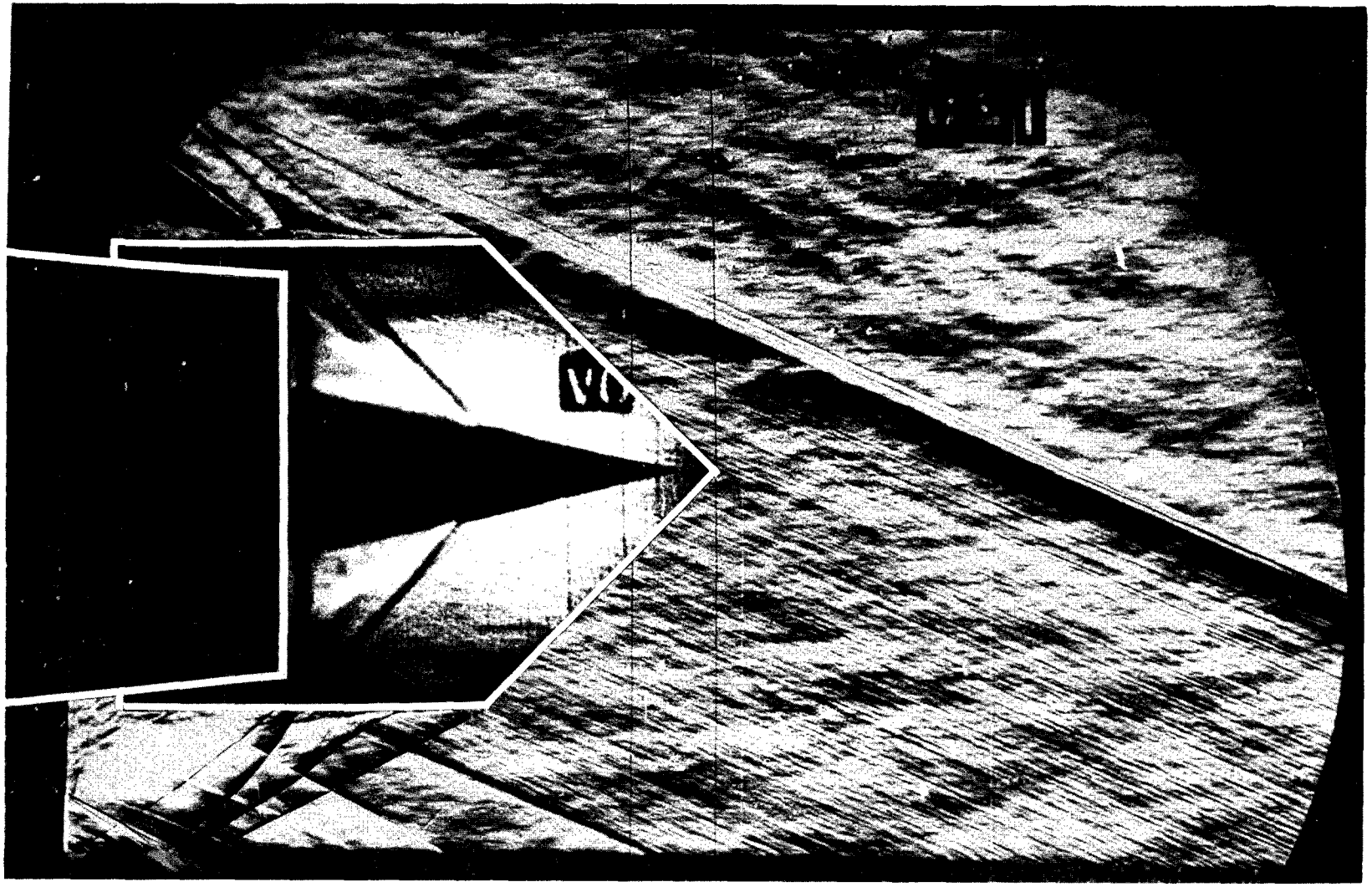

(b) Splitter plate 3.

L-66-1006

Figure 11.- Continued.

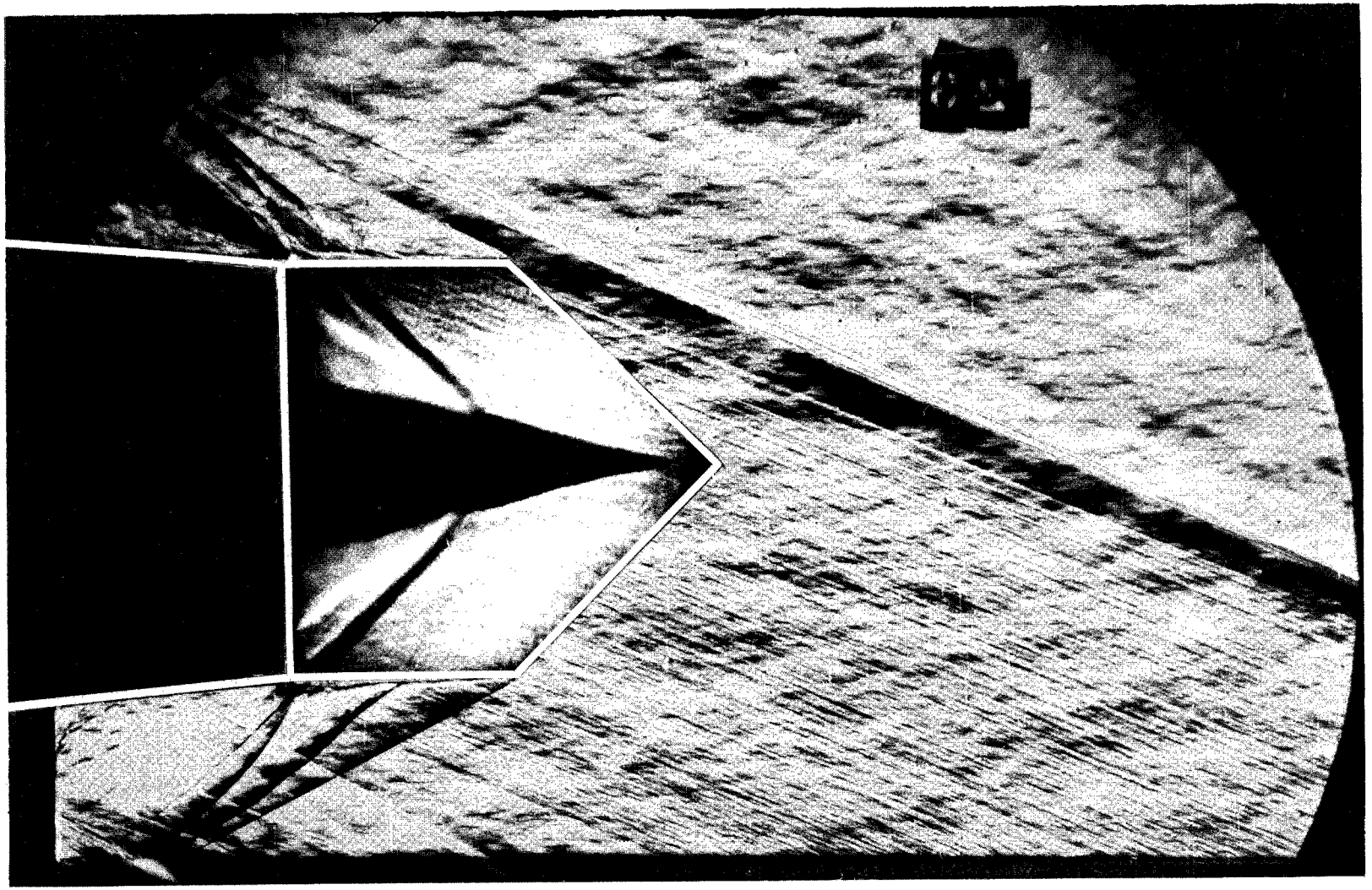

(c) Splitter plate 4. L-66-1007

Figure 11.- Concluded.

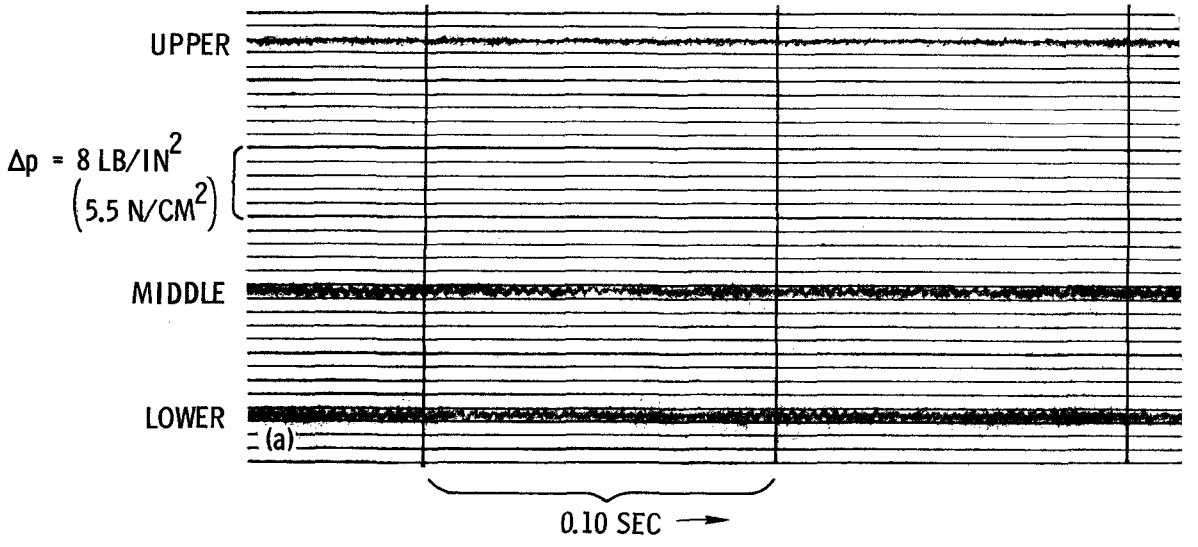

(a) Splitter plate 1.

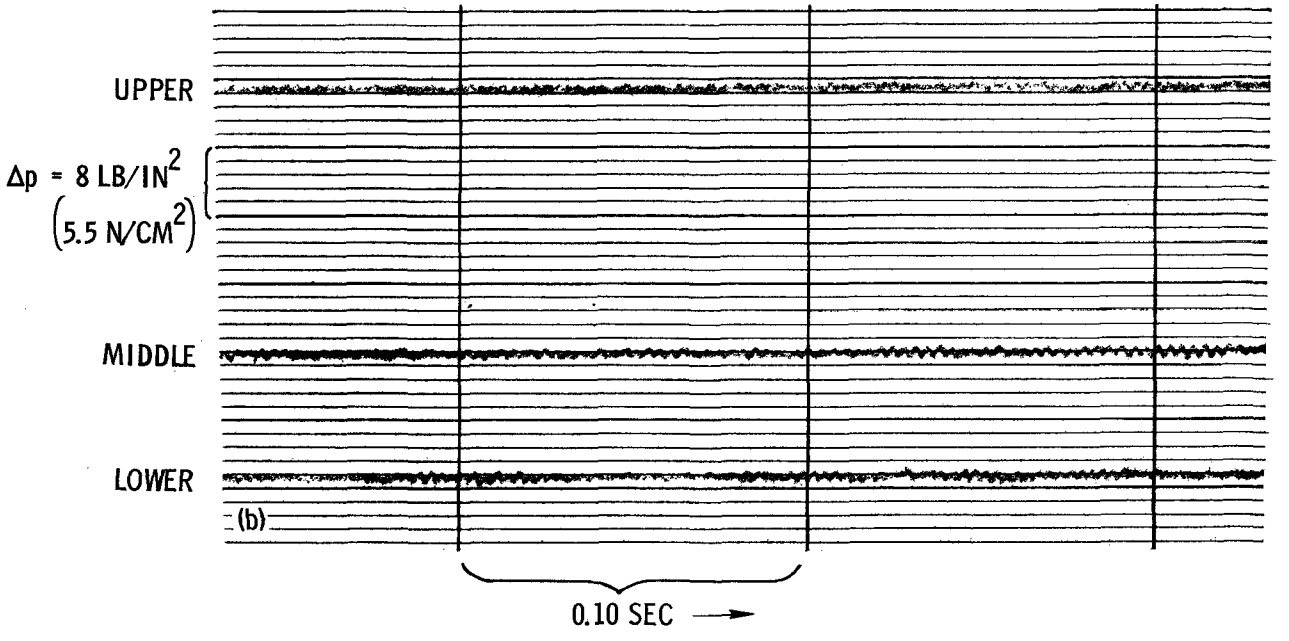

(b) Splitter plate 2.

Figure 12.- Pressure traces. High pylon; $\psi = 0^0$; $\dot{m}_2/\dot{m}_1 = 0.72$.

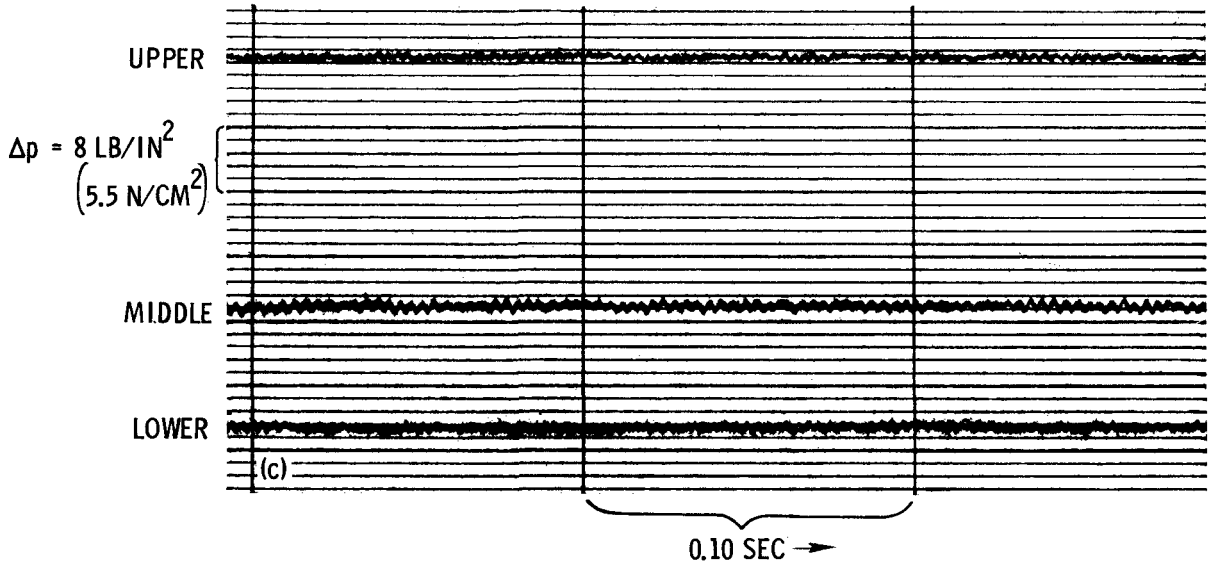

(c) Splitter plate 3.

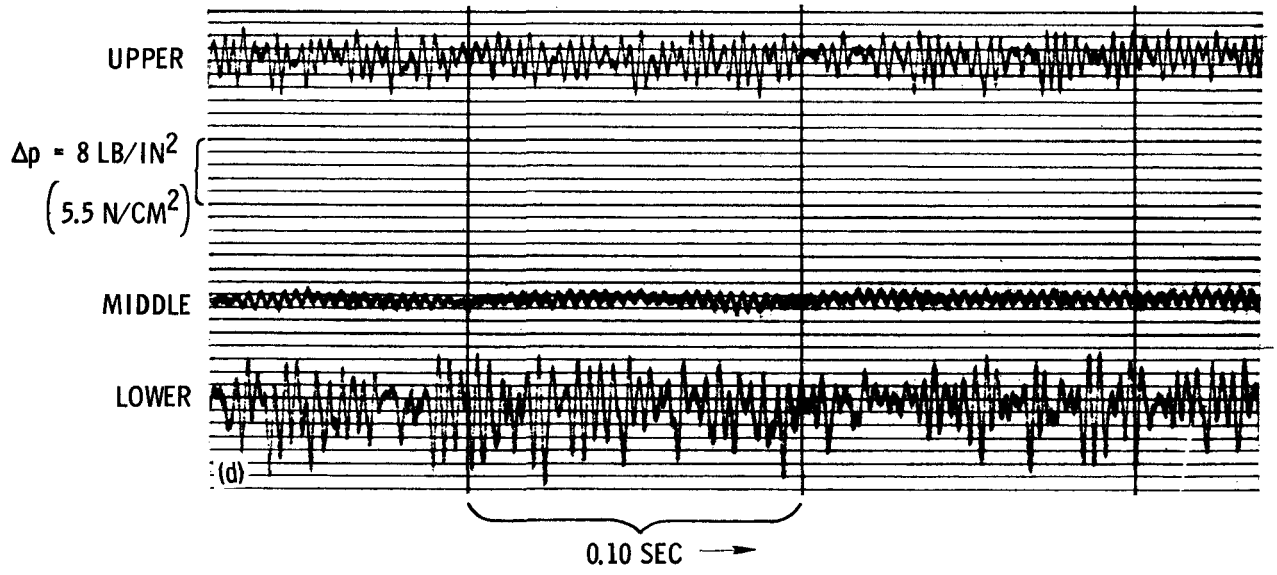

(d) Splitter plate 4.

Figure 12.- Concluded.

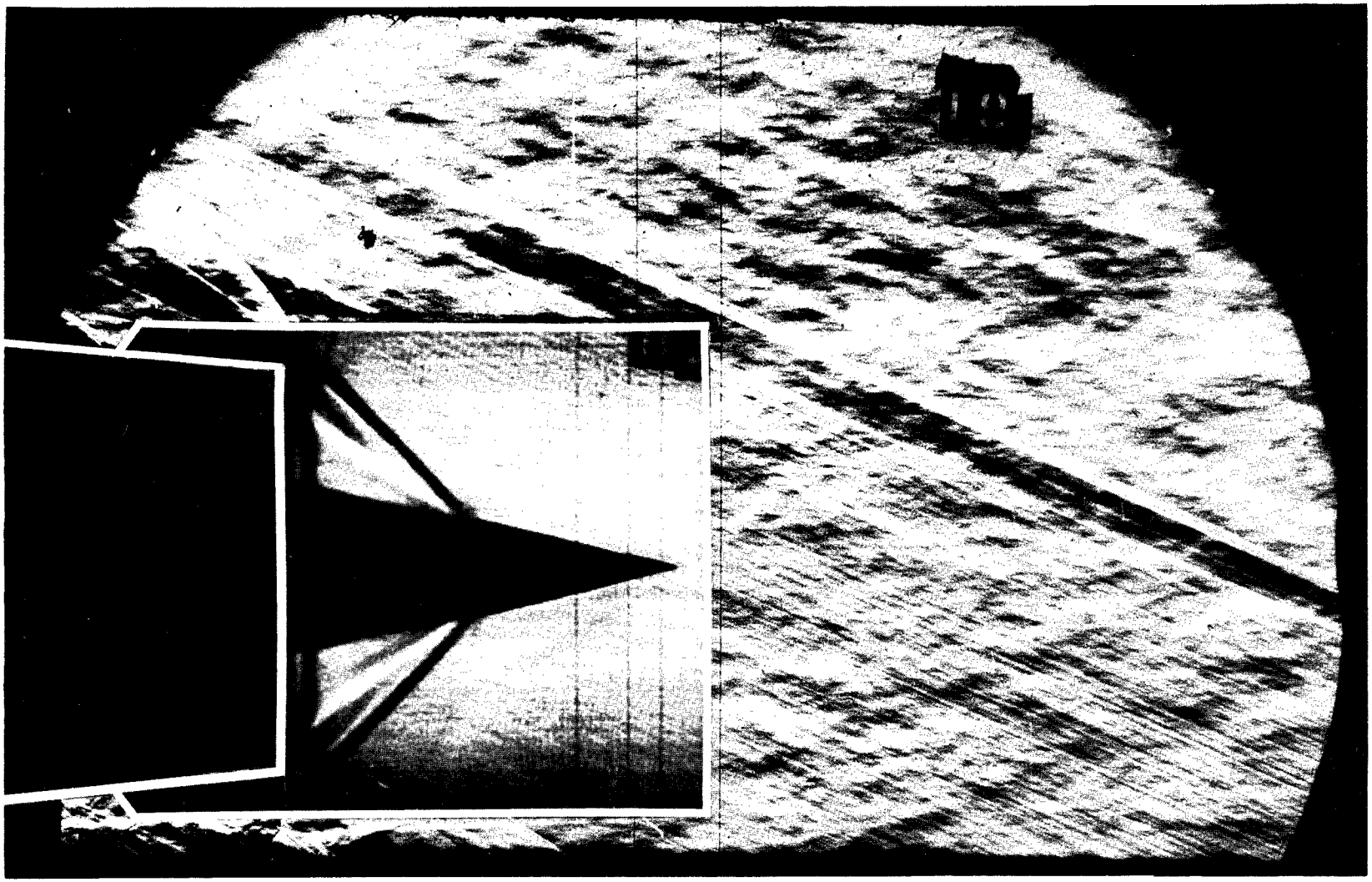

(a) Splitter plate 1.

Figure 13.- Composite shadowgraph and schlieren of the flow. Medium pylon; $\psi = 0^{0}$; $\dot{m}_2/\dot{m}_1 = 0.72$.

L-66-1008

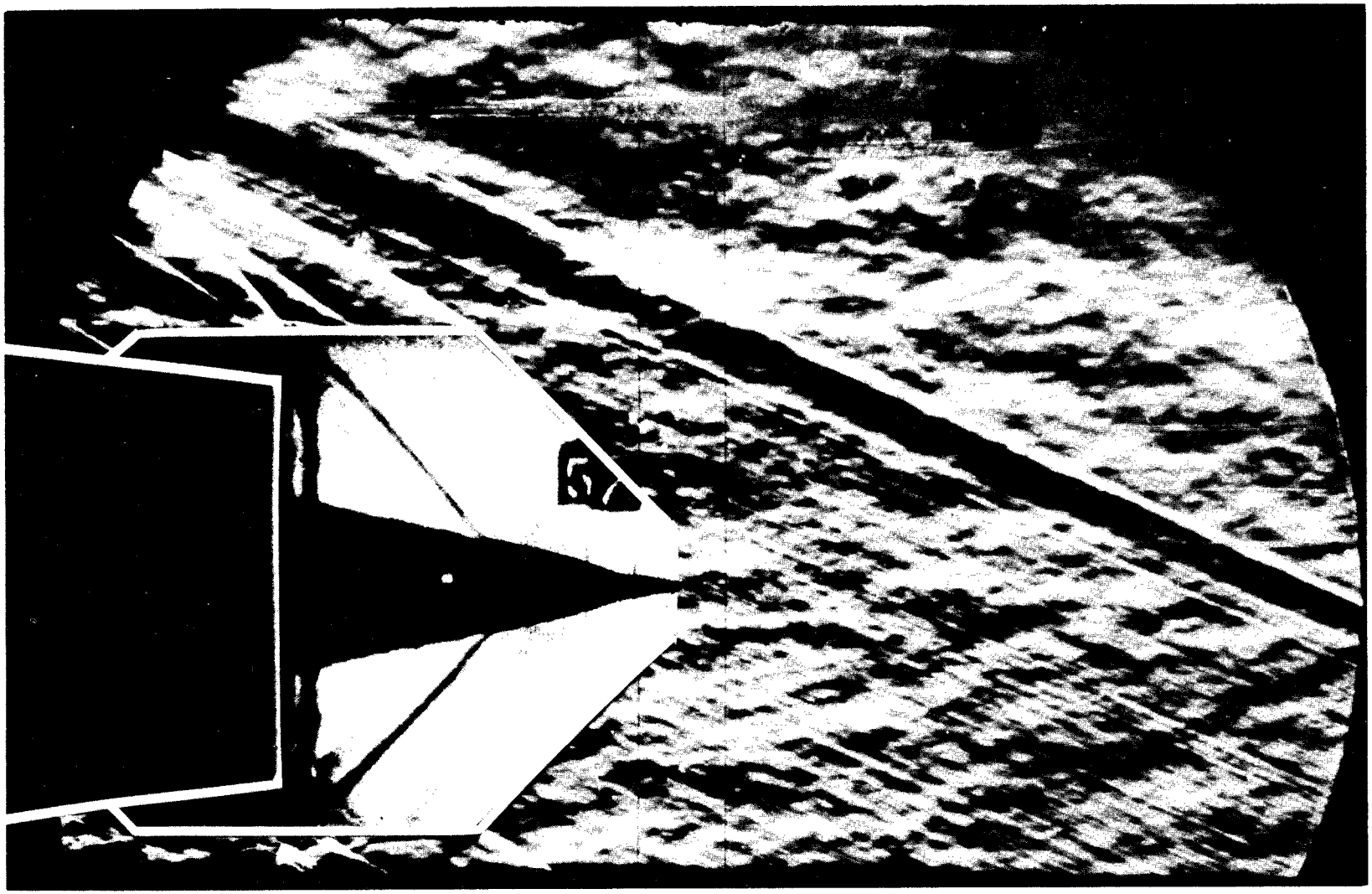

(b) Splitter plate 2.

L-66-1009

Figure 13.- Continued.

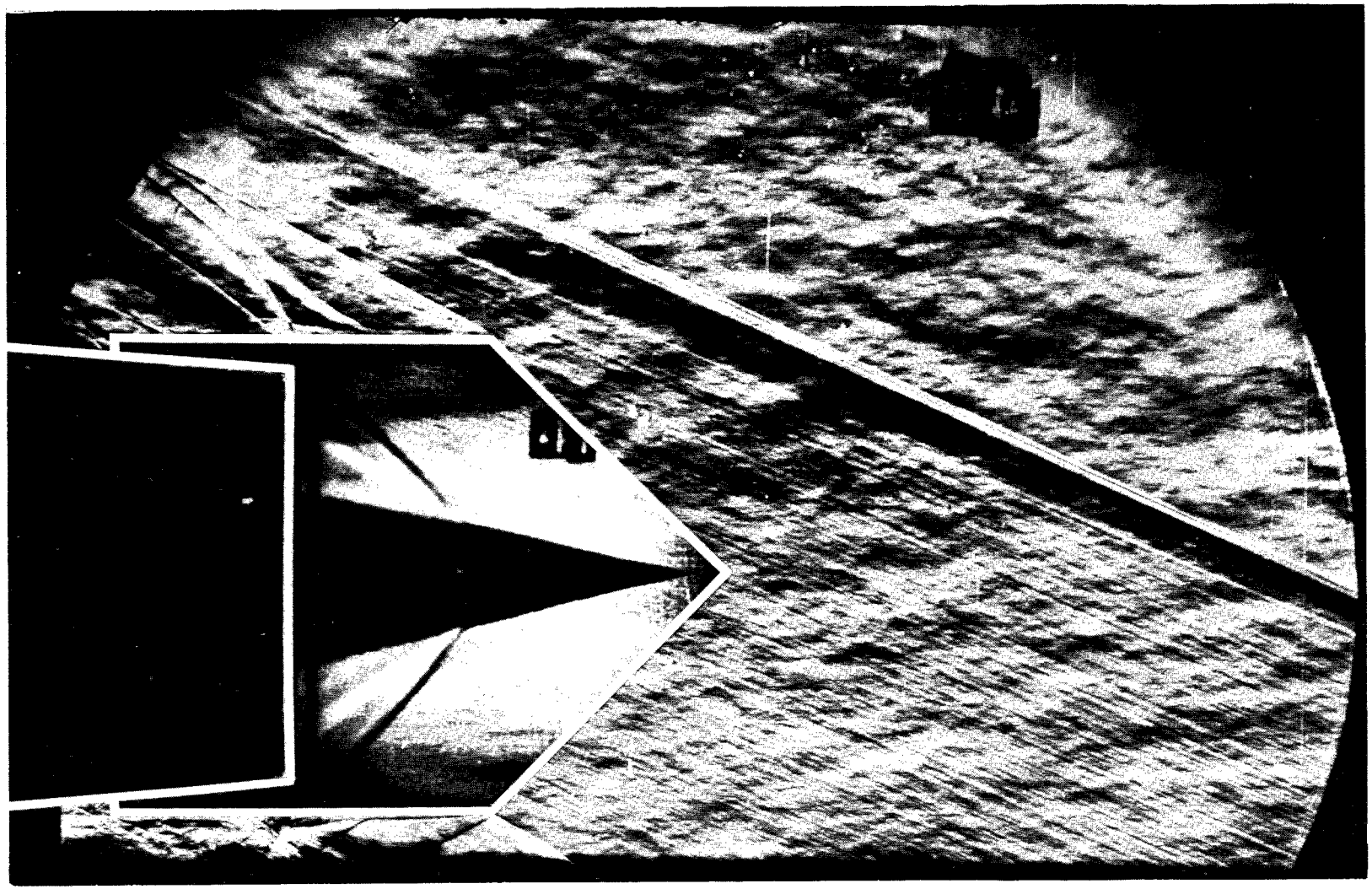

(c) Splitter plate 3.

L-66-1010

Figure 13.- Concluded.

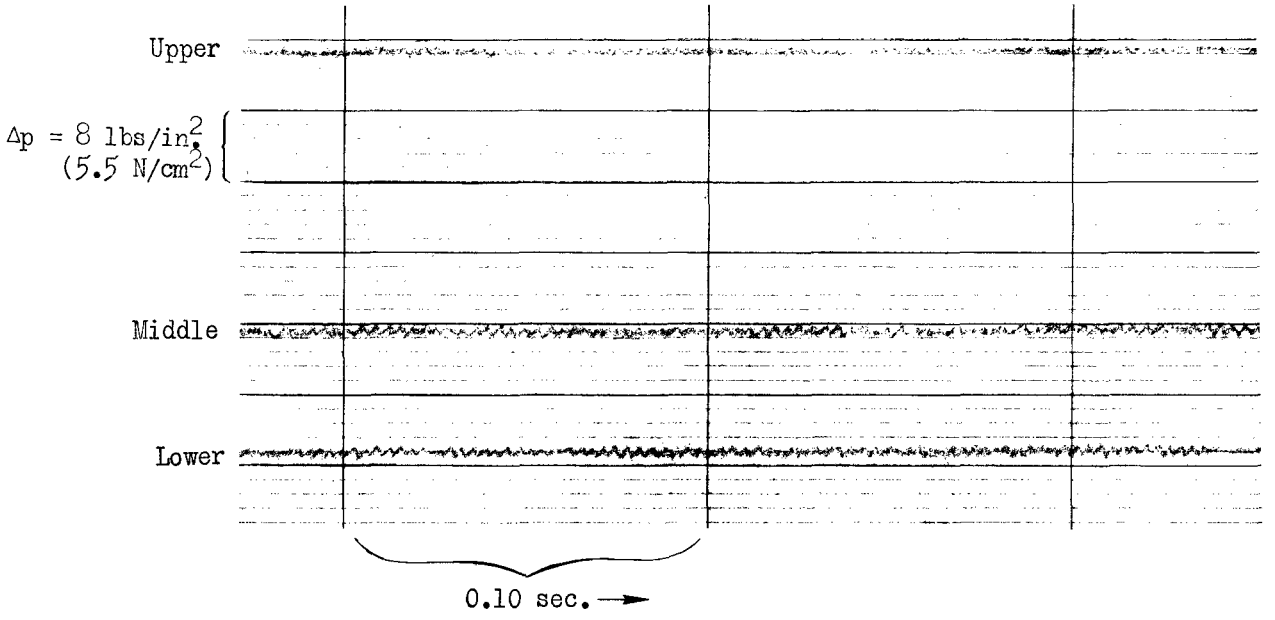

(a) Splitter plate 1.

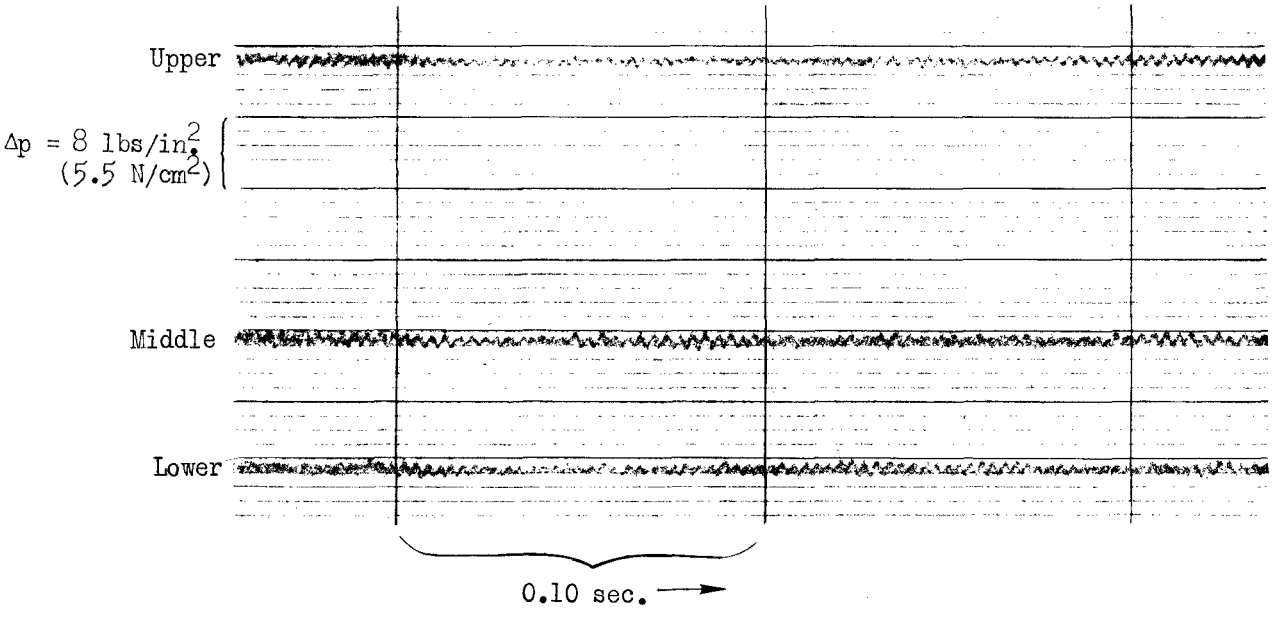

(b) Splitter plate 2.

Figure 14.- Pressure traces. Medium pylon; $\psi = 0^{o}$; $\dot{m}_2/\dot{m}_1 = 0.72$.

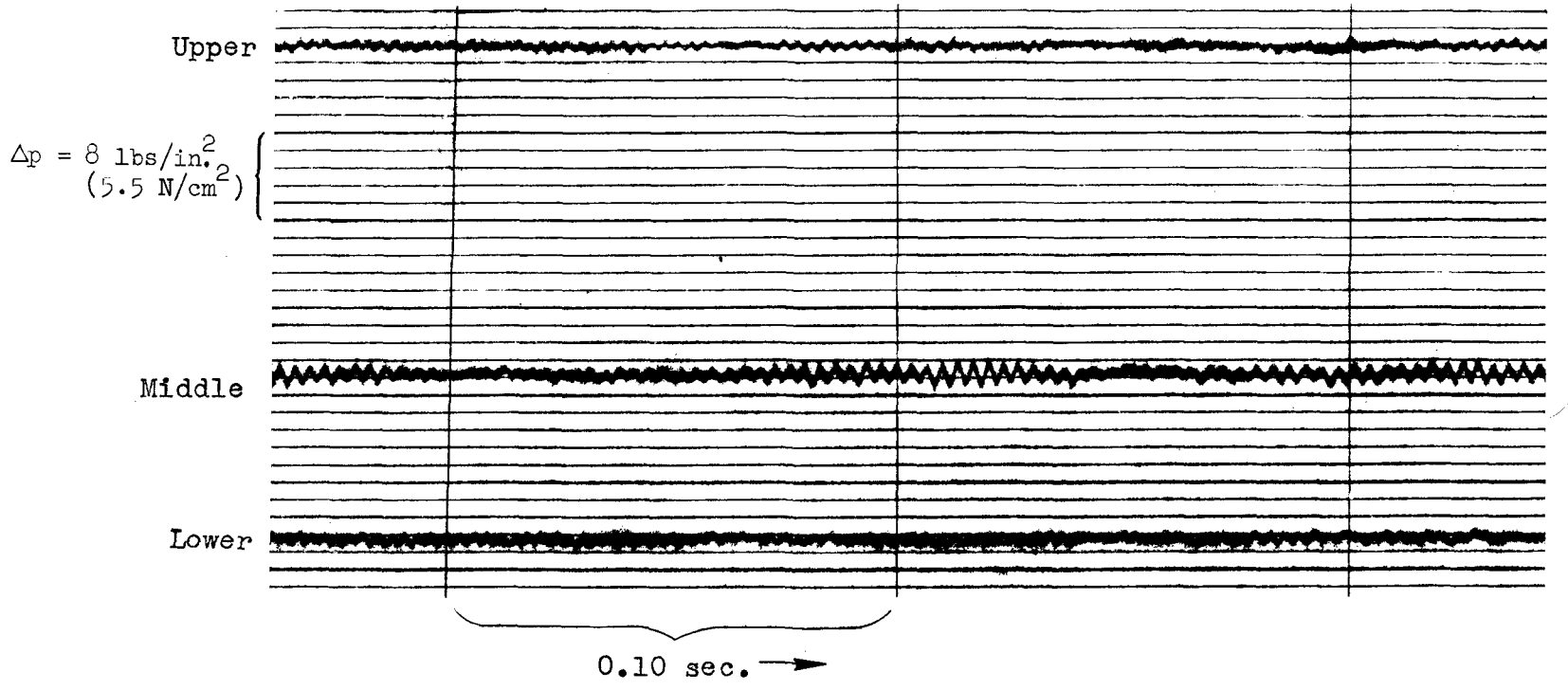

(c) Splitter plate 3.

Figure 14.- Concluded.

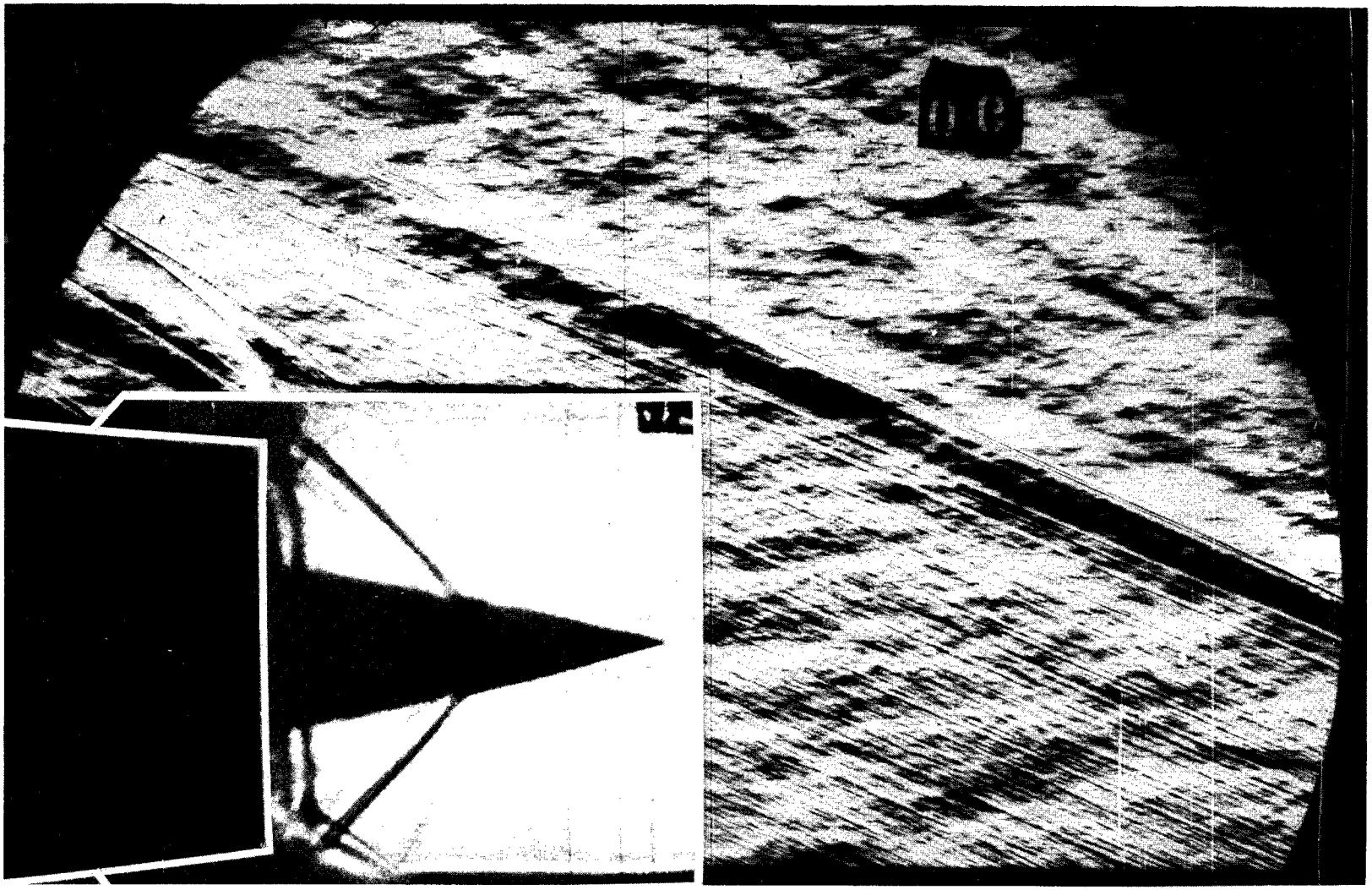

(a) Splitter plate 1.

L-66-1011

Figure 15.- Composite shadowgraph and schlieren of the flow. Low pylon; $\psi = 0^0$; $\dot{m}_2/\dot{m}_1 = 0.71$.

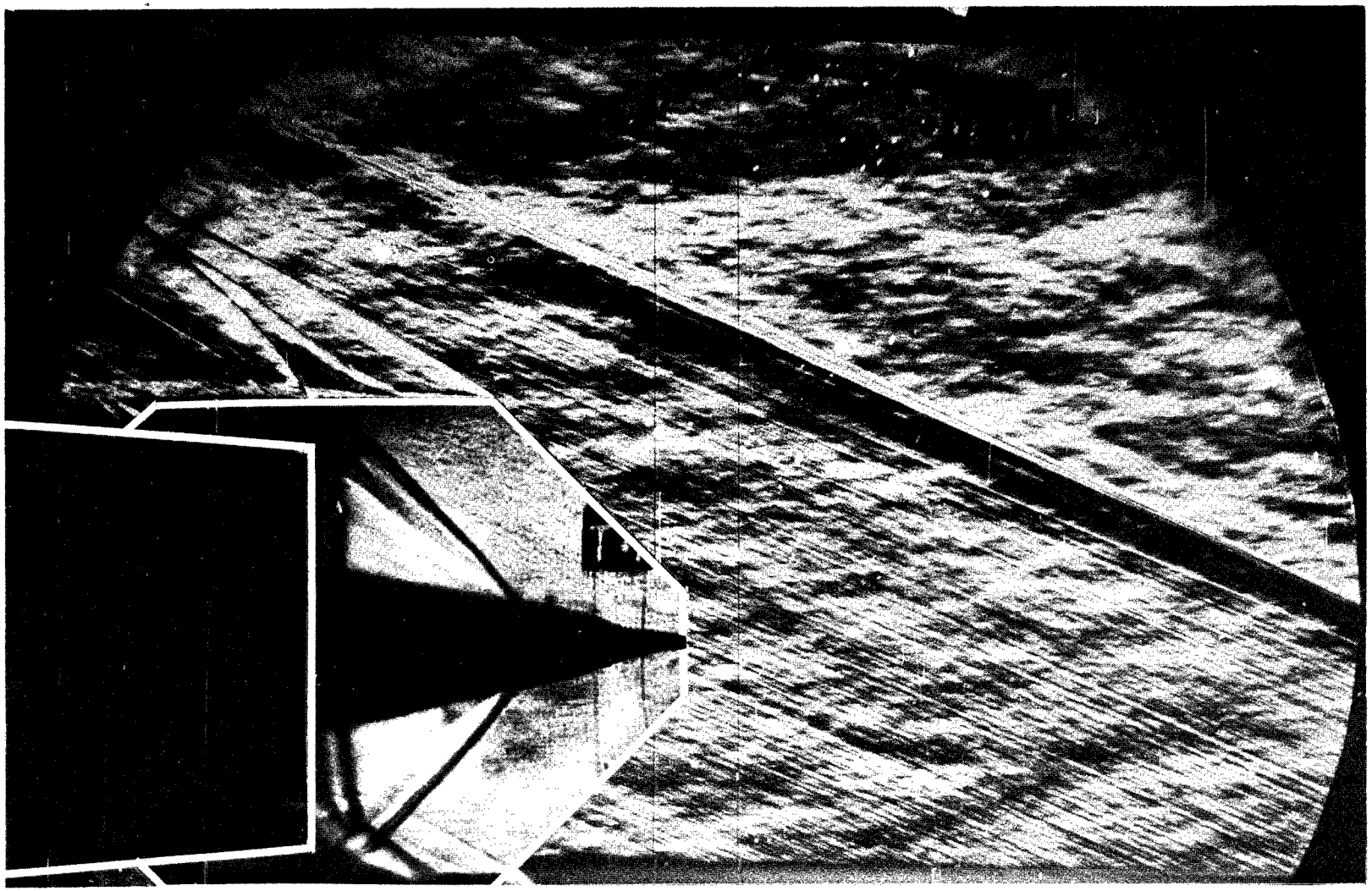

(b) Splitter plate 2. L-66-1012

Figure 15.- Continued.

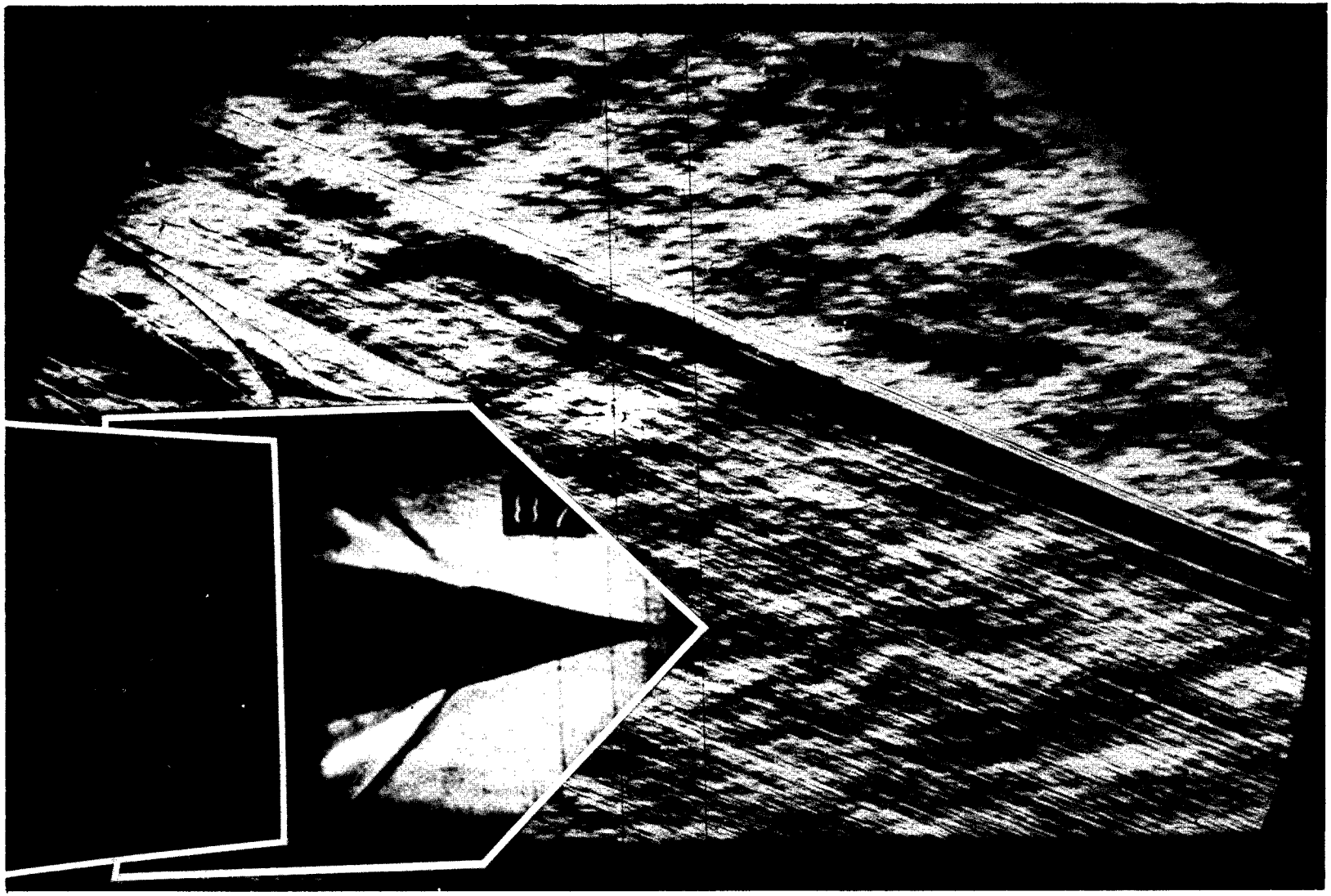

(c) Splitter plate 3. L-66-1013

Figure 15.- Concluded.

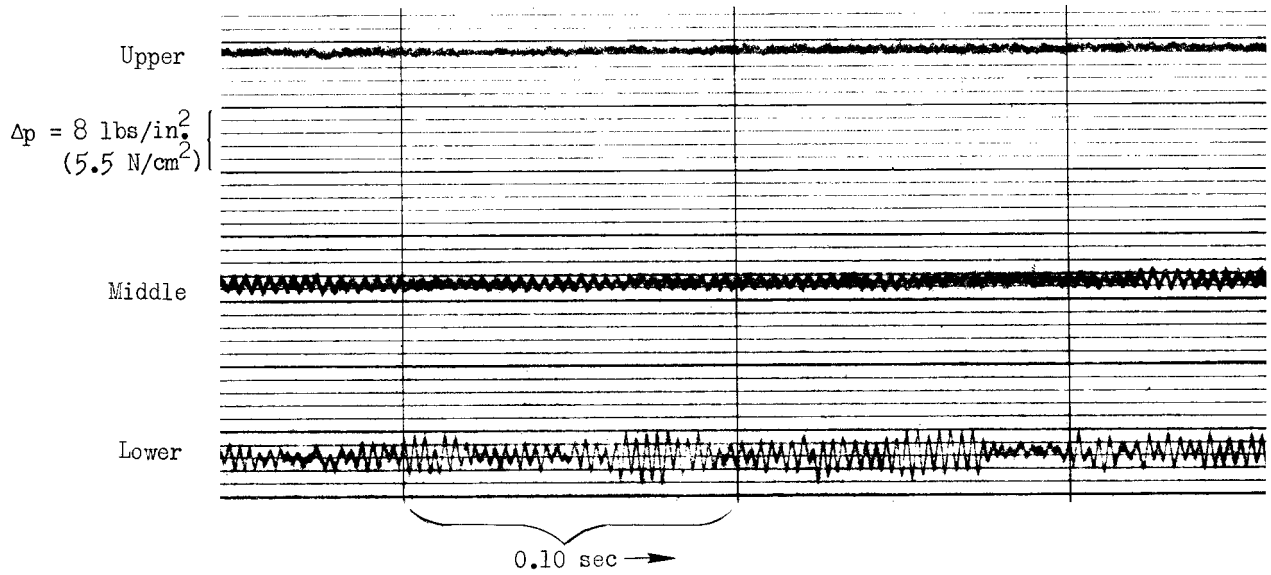

(a) Splitter plate 1.

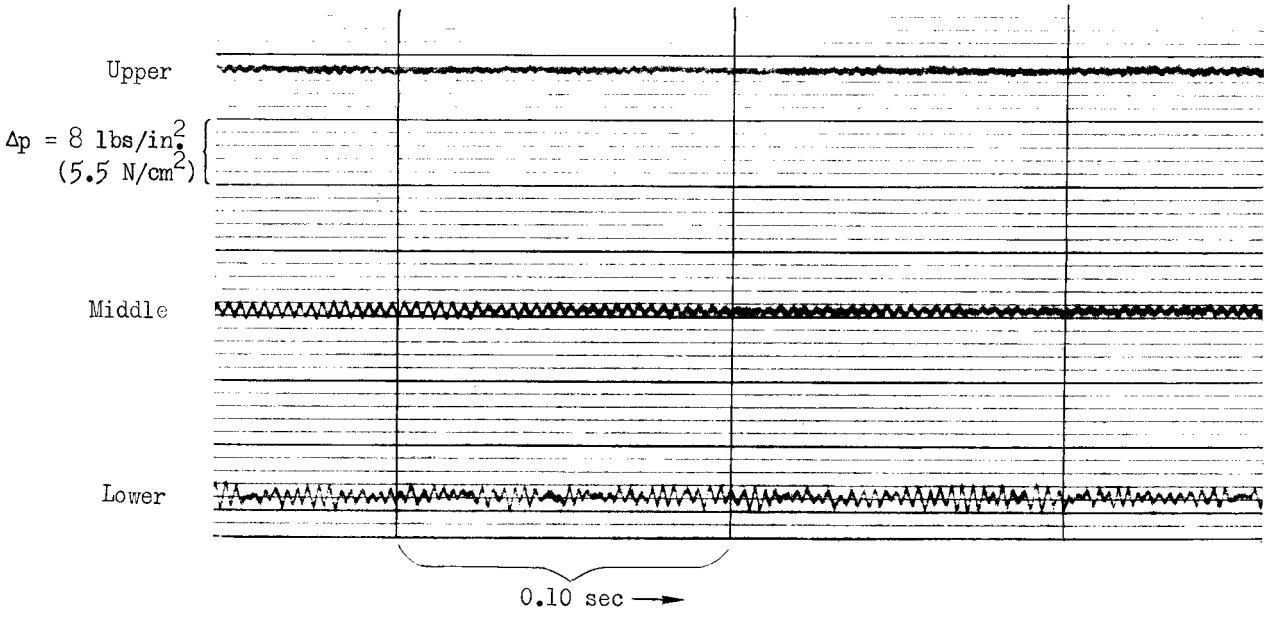

(b) Splitter plate 2.

Figure 16.- Pressure traces. Low pylon; $\psi = 0^{o}$; $\dot{m}_2/\dot{m}_1 = 0.71$.

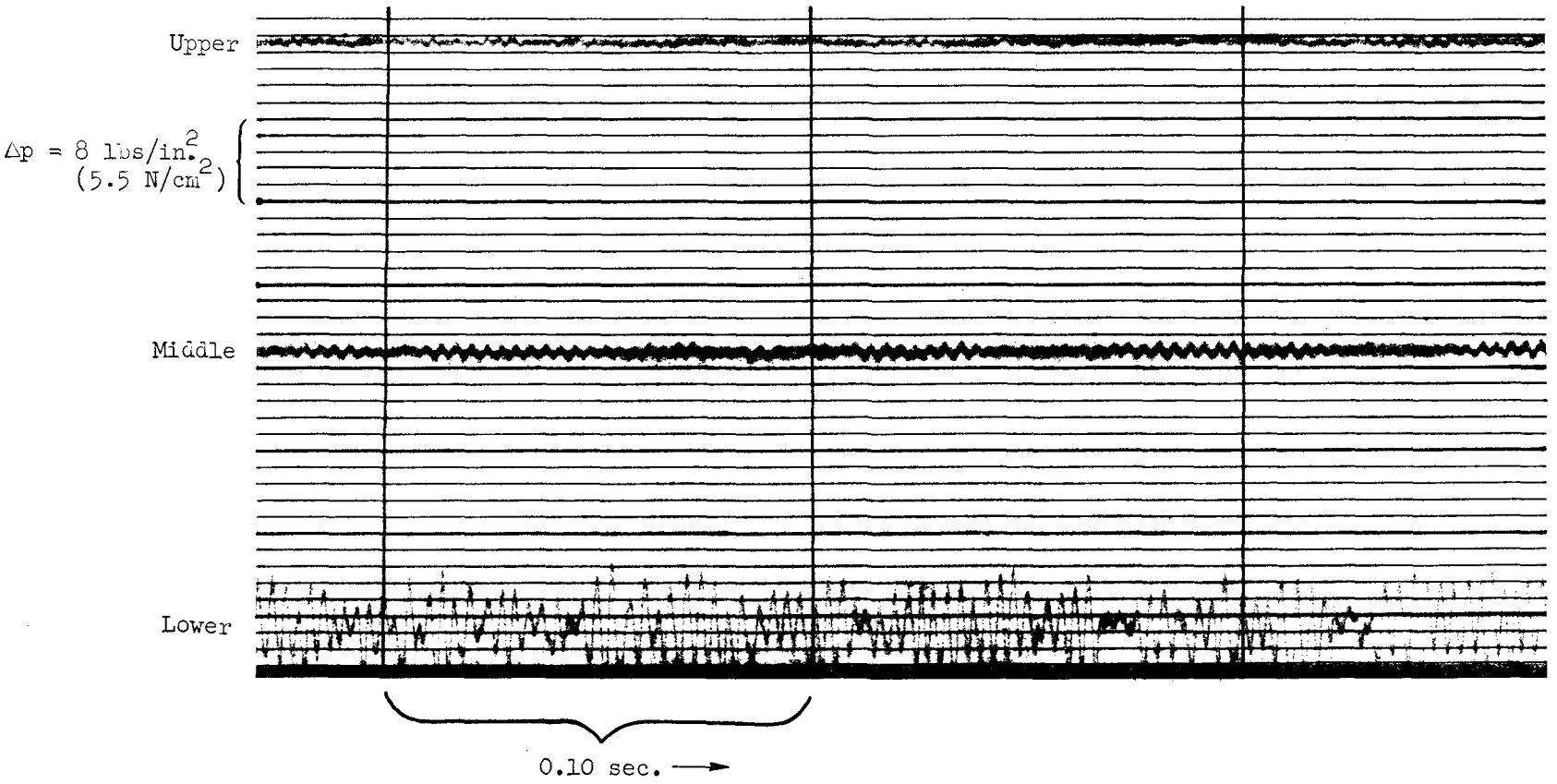

(c) Splitter plate 3.

Figure 16.- Concluded.

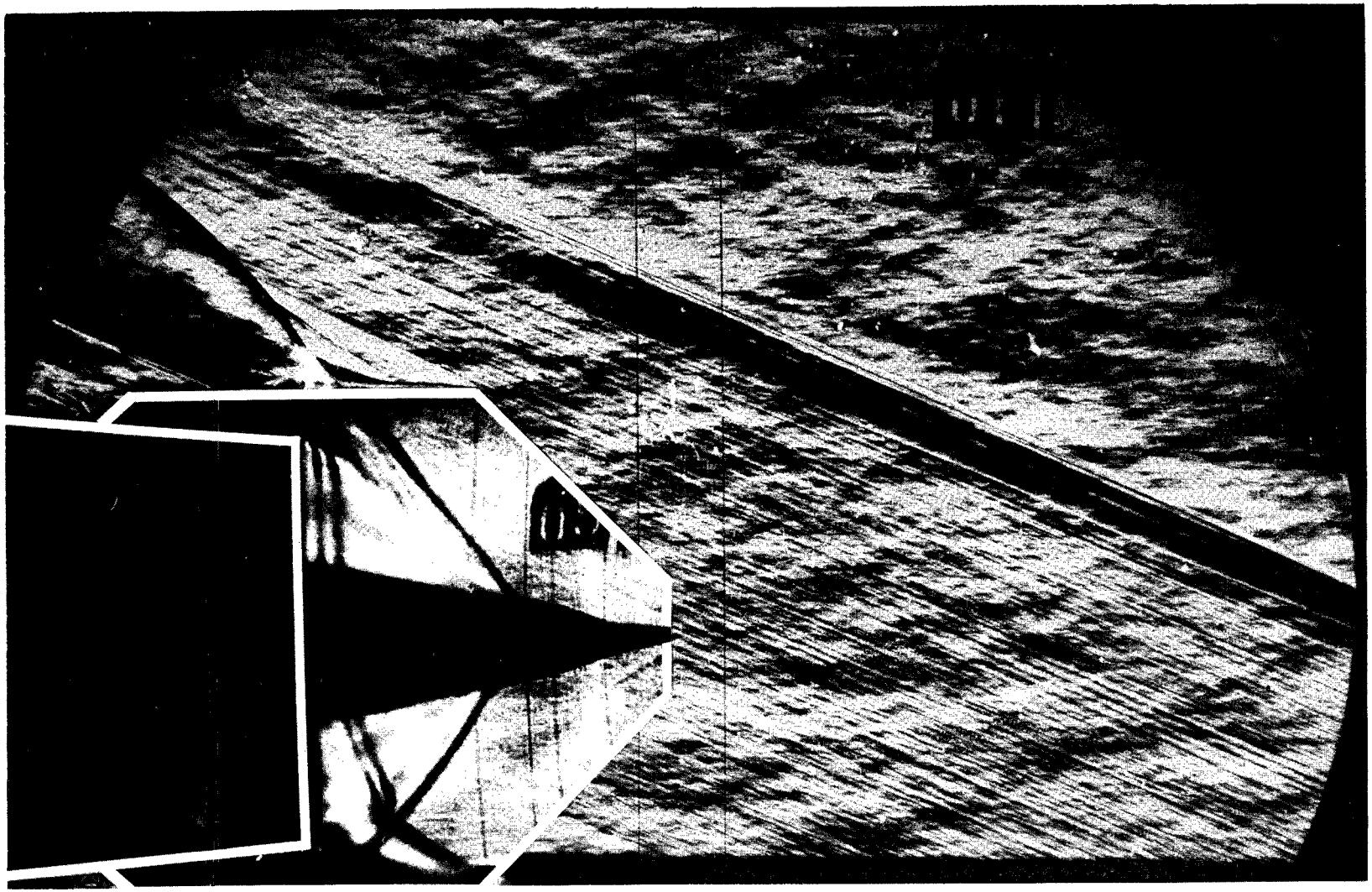

(a) Splitter plate 2; low pylon.

L-66-1014

Figure 17.- Composite shadowgraph and schlieren of the flow. $\psi = 6^{0}$; $\dot{m}_2/\dot{m}_1 = 0.62$.

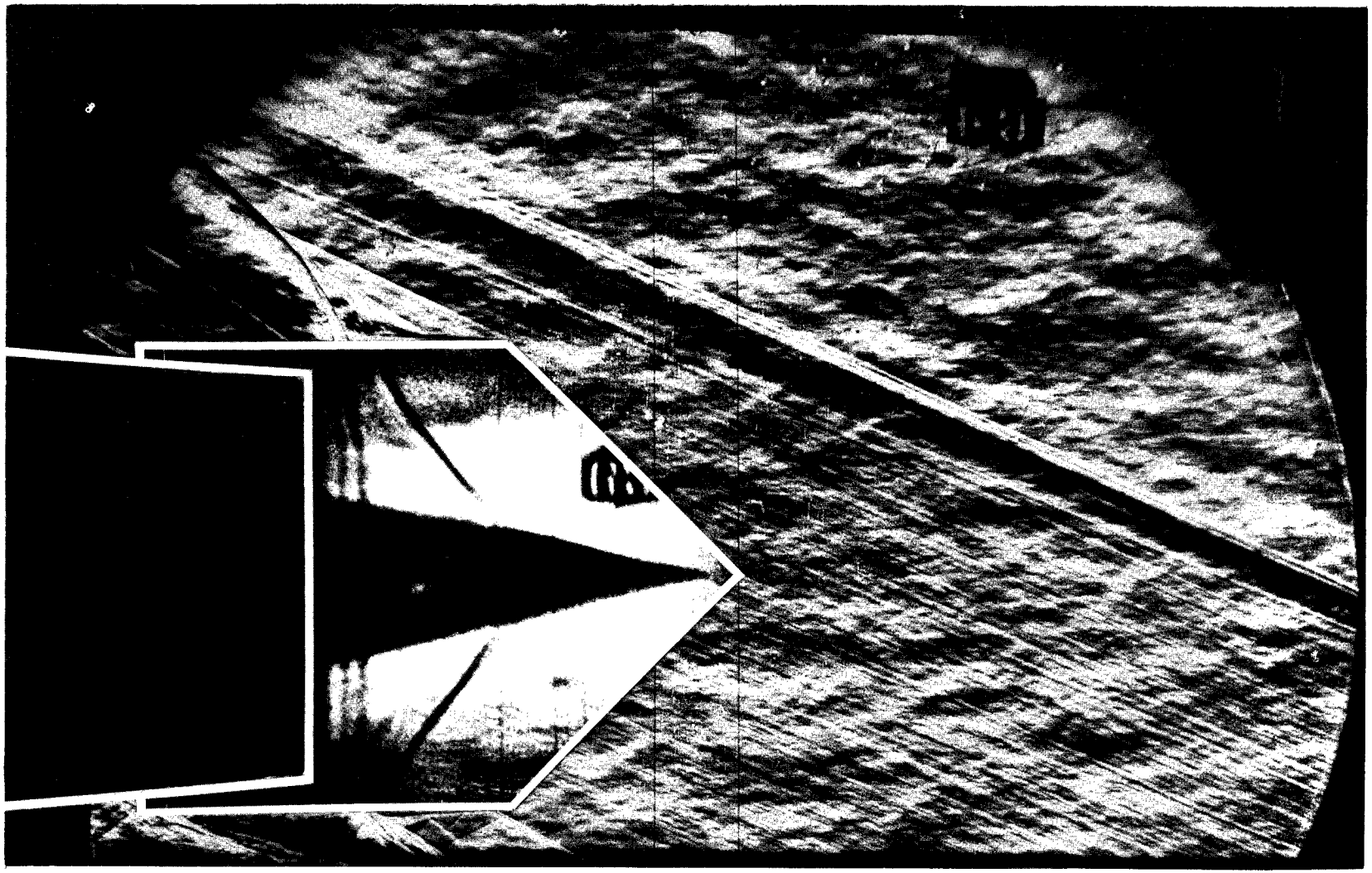

(b) Splitter plate 3; medium pylon. L-66-1015

Figure 17.- Concluded.

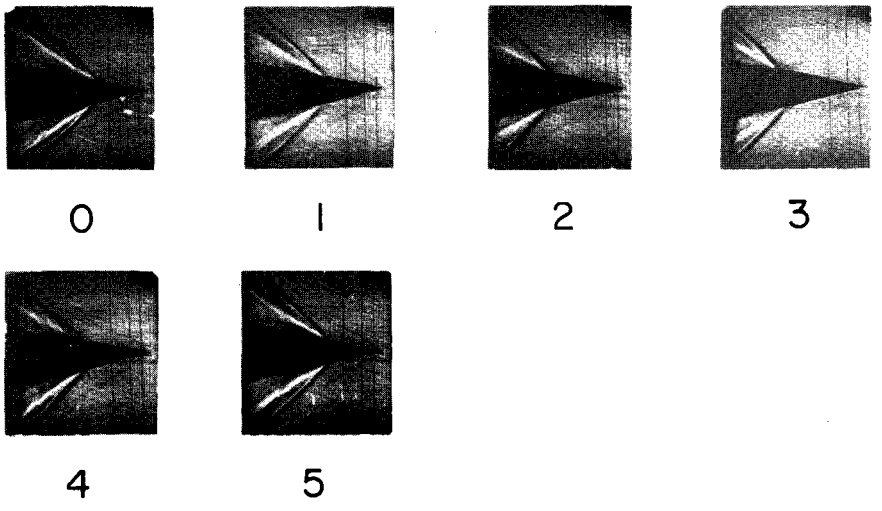

(a) $\dot{m}_2/\dot{m}_1 = 0.65$.

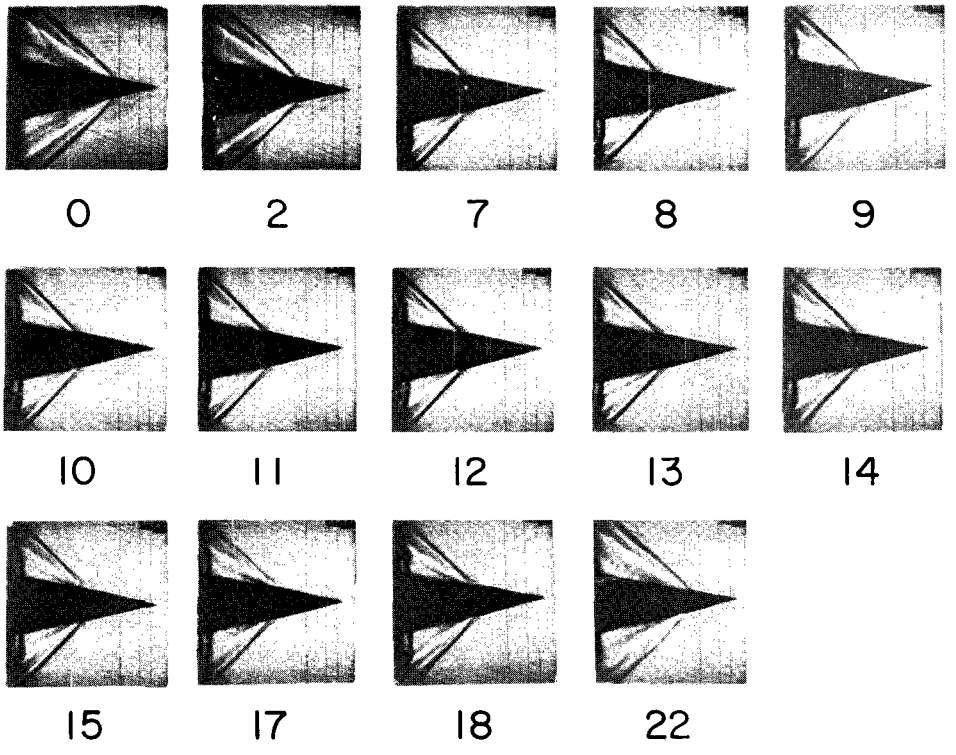

(b) $\dot{m}_2/\dot{m}_1 = 0.63$.

Figure 18.- Shadowgraphs of the flow. 2,000 frames/sec; splitter plate 1; $\psi = 0^{\circ}$; high or medium pylon. L-66-1016

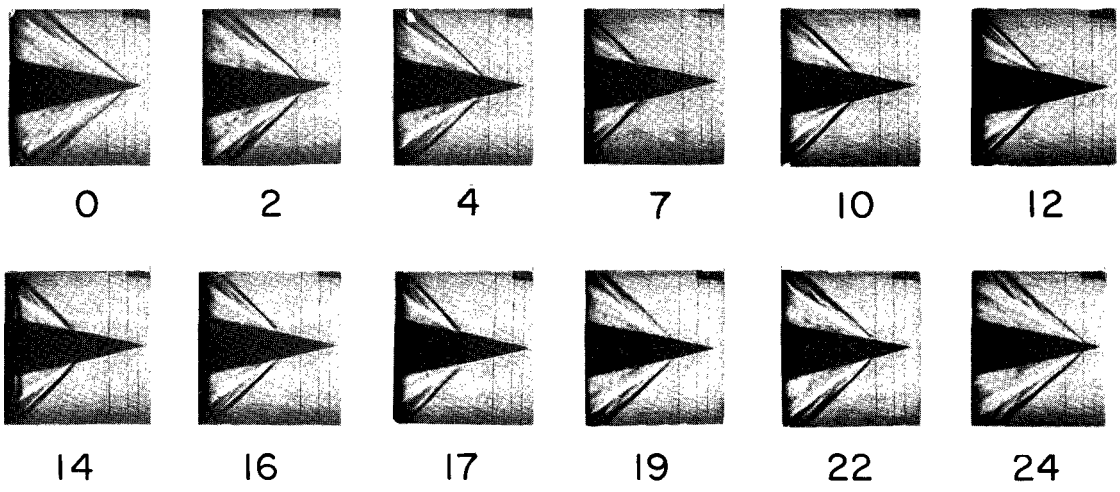

(c) $\dot{m}_2/\dot{m}_1 = 0.57$.

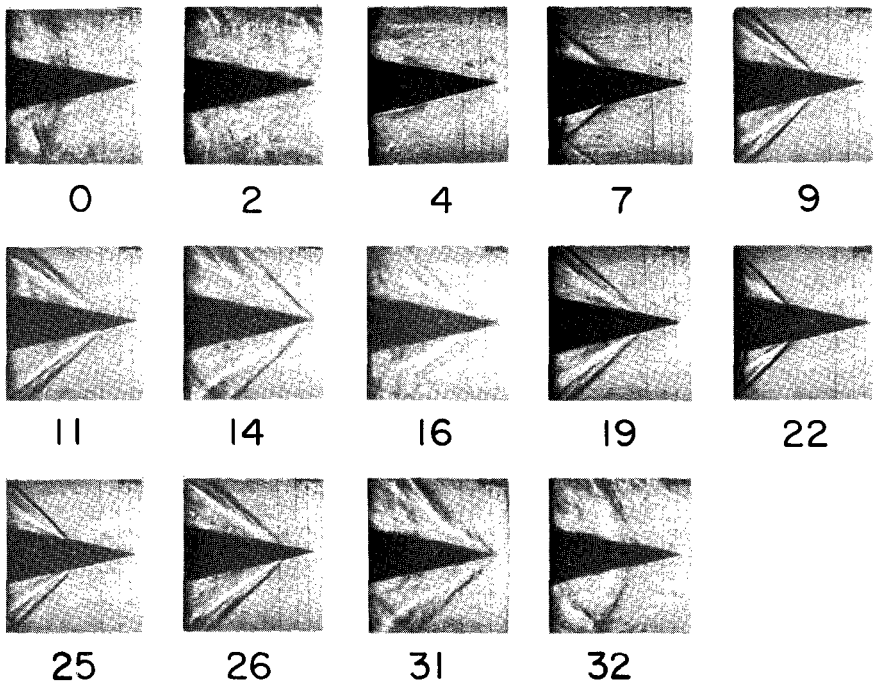

(d) $\dot{m}_2/\dot{m}_1 = 0.44$.

L-66-1017

Figure 18.- Concluded.

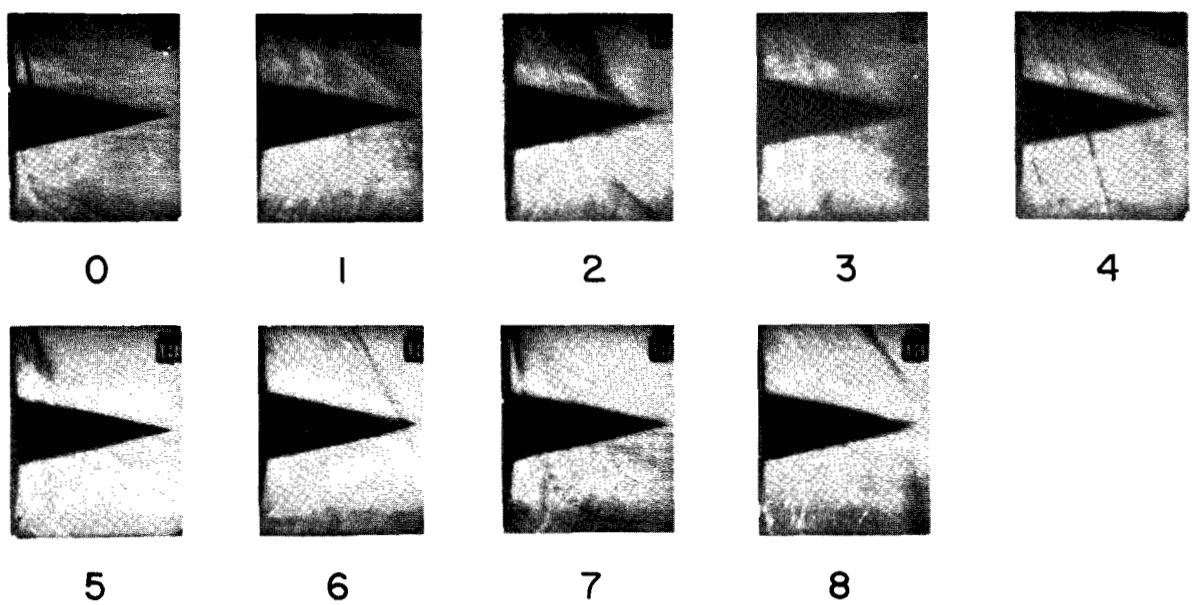

Figure 19.- Shadowgraphs of the flow. 750 frames/sec; splitter plate 1; high pylon; $\psi = 0^0$; $\dot{m}_2/\dot{m}_1 = 0$. L-66-1018

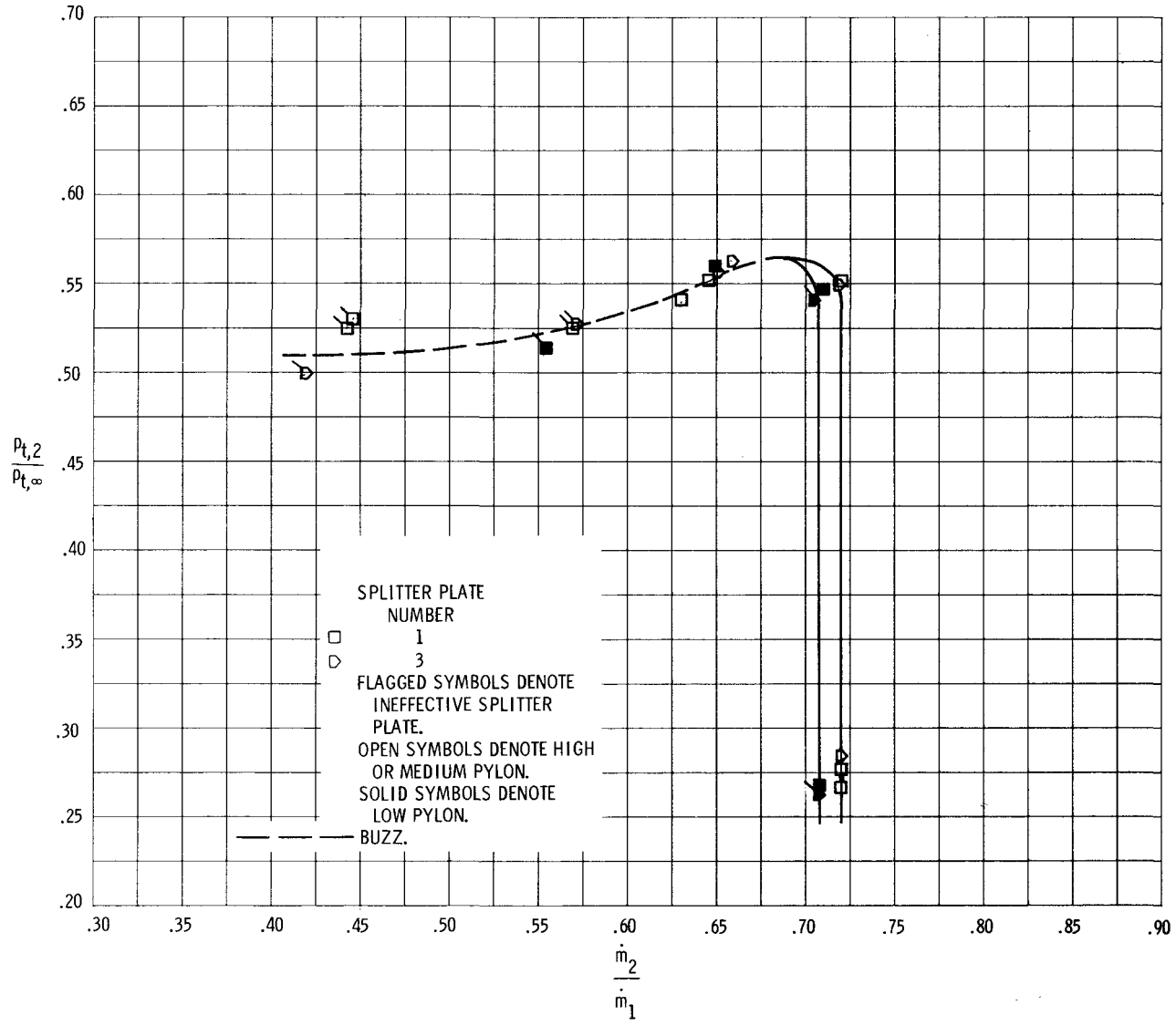

(a) Splitter plates 1 and 3.

Figure 20.- Variation of pressure recovery with mass-flow ratio. $\psi = 0^{o}$.

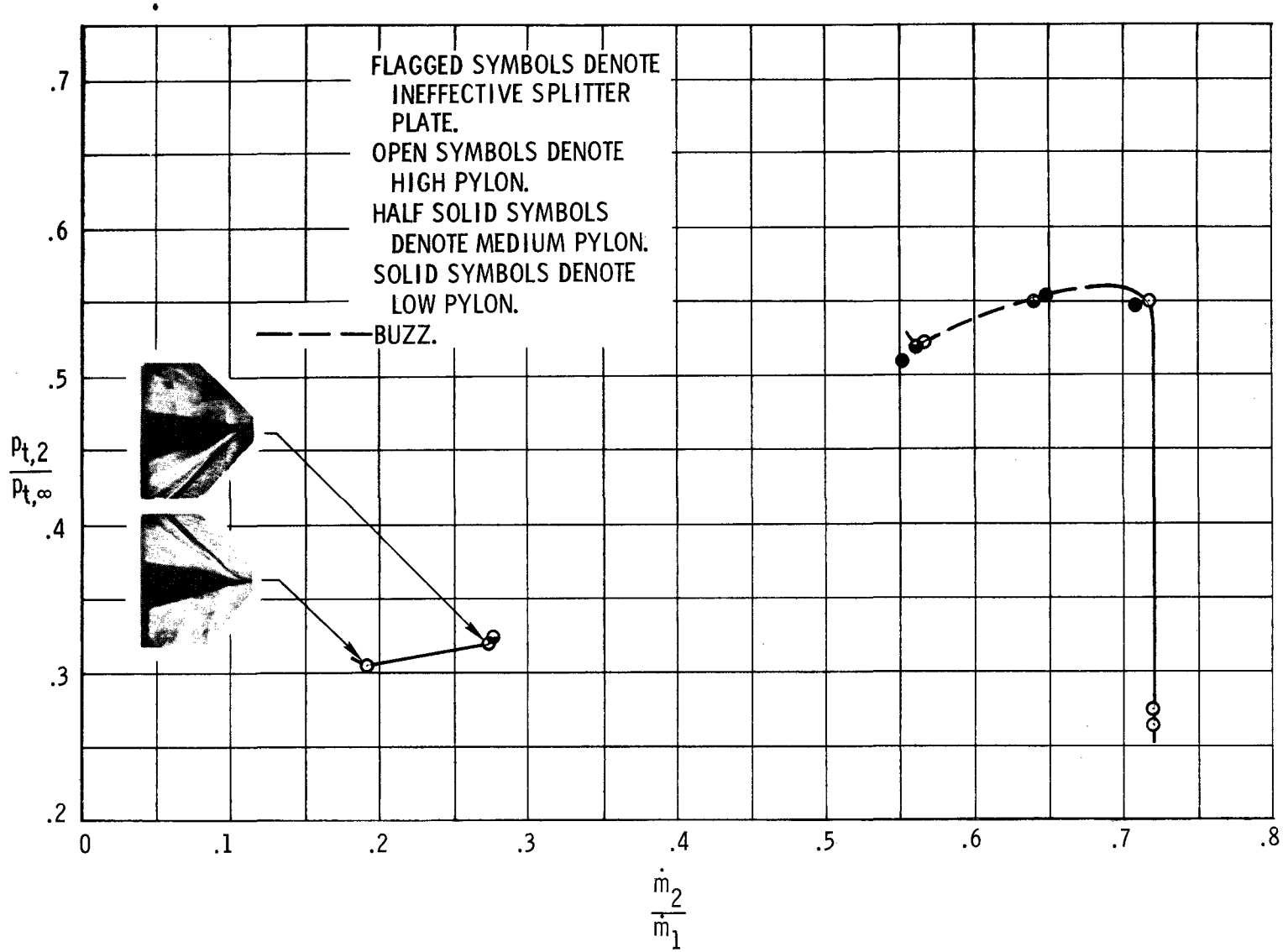

(b) Splitter plate 2.

Figure 20.- Concluded.

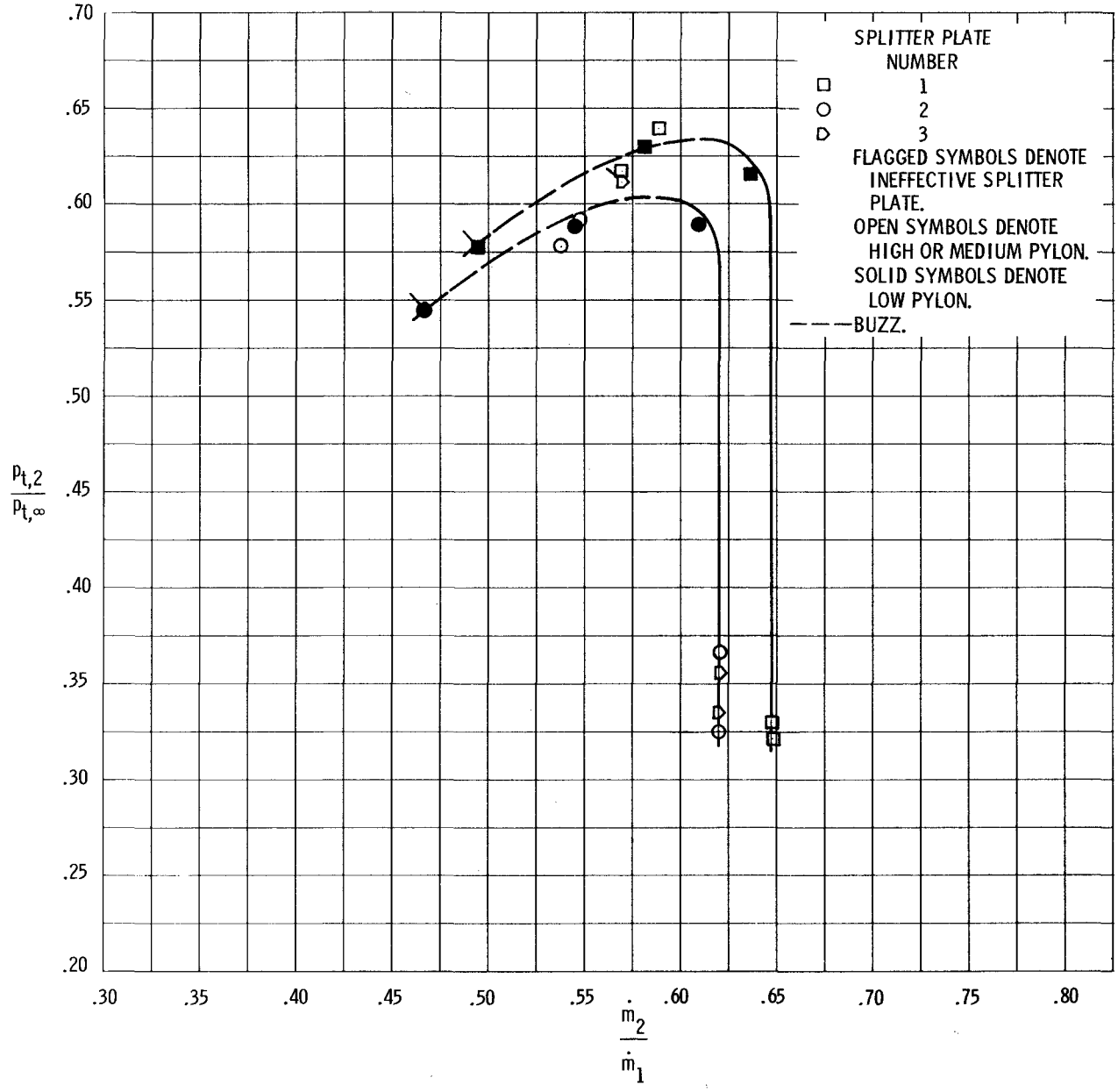

Figure 21.- Variation of pressure recovery with mass-flow ratio. $\psi = 6^0$.

NASA-Langley, 1966 L-4729

"The aeronautical and space activities of the United States shall be conducted so as to contribute . . . to the expansion of human knowledge of phenomena in the atmosphere and space. The Administration shall provide for the widest practicable and appropriate dissemination of information concerning its activities and the results thereof."

—NATIONAL AERONAUTICS AND SPACE ACT OF 1958

NASA SCIENTIFIC AND TECHNICAL PUBLICATIONS

TECHNICAL REPORTS: Scientific and technical information considered important, complete, and a lasting contribution to existing knowledge.

TECHNICAL NOTES: Information less broad in scope but nevertheless of importance as a contribution to existing knowledge.

TECHNICAL MEMORANDUMS: Information receiving limited distribution because of preliminary data, security classification, or other reasons.

CONTRACTOR REPORTS: Technical information generated in connection with a NASA contract or grant and released under NASA auspices.

TECHNICAL TRANSLATIONS: Information published in a foreign language considered to merit NASA distribution in English.

TECHNICAL REPRINTS: Information derived from NASA activities and initially published in the form of journal articles.

SPECIAL PUBLICATIONS: Information derived from or of value to NASA activities but not necessarily reporting the results of individual NASA-programmed scientific efforts. Publications include conference proceedings, monographs, data compilations, handbooks, sourcebooks, and special bibliographies.

Details on the availability of these publications may be obtained from:

SCIENTIFIC AND TECHNICAL INFORMATION DIVISION

NATIONAL AERONAUTICS AND SPACE ADMINISTRATION

Washington, D.C. 20546